

Exquisite Selectivity for Human Toll-Like Receptor 8 in Substituted Furo[2,3-*c*]quinolines

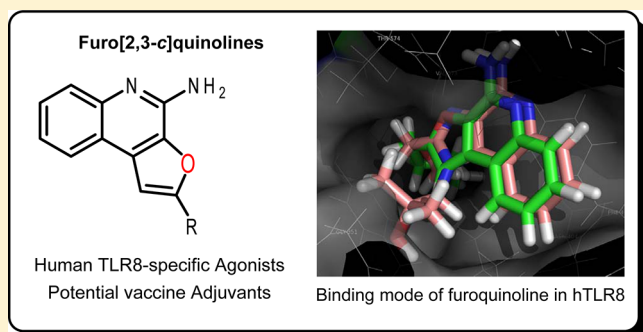
Hari Prasad Kokatla,[†] Diptesh Sil,[†] Subbalakshmi S. Malladi,[†] Rajalakshmi Balakrishna,[†] Alec R. Hermanson,[†] Lauren M. Fox,[†] Xinkun Wang,[‡] Anshuman Dixit,[§] and Sunil A. David*,[†]

[†]Department of Medicinal Chemistry and [‡]Genomics Facility, University of Kansas, Lawrence, Kansas 66047, United States

[§]Department of Translational Research and Technology Development, Institute of Life Sciences, Nalco Square, Bhubaneswar 751023, India

Supporting Information

ABSTRACT: Toll-like receptor (TLR)-8 agonists activate adaptive immune responses by inducing robust production of T helper 1-polarizing cytokines, suggesting that TLR8-active compounds may be promising candidate adjuvants. We synthesized and evaluated hitherto unexplored furo[2,3-*c*]quinolines and regiosomeric furo[3,2-*c*]quinolines derived via a tandem, one-pot Sonogashira coupling and intramolecular *S*-endo-dig cyclization strategy in a panel of primary screens. We observed a pure TLR8-agonistic activity profile in select furo[2,3-*c*]quinolines, with maximal potency conferred by a C2-butyl group ($EC_{50} = 1.6 \mu\text{M}$); shorter, longer, or substituted homologues as well as compounds bearing C1 substitutions were inactive, which was rationalized by docking studies using the recently described crystal structure of human TLR8. The best-in-class compound displayed prominent proinflammatory cytokine induction (including interleukin-12 and interleukin-18), but was bereft of interferon- α inducing properties, confirming its high selectivity for human TLR8.



INTRODUCTION

Vaccines have played an indispensable role in the dramatic improvement in public health witnessed in modern times, particularly in the prevention of mortality and morbidity attributable to infectious diseases.¹ Although the successes of active immunization beginning with Jenner's smallpox vaccine in 1796 are numerous and extraordinary, our failure to develop effective vaccines against diseases such as the human immunodeficiency virus (HIV), tuberculosis, and malaria have served to highlight the deficiencies and shortcomings of state-of-the-art contemporary vaccine technology, catalyzing a renaissance in rational vaccine design and development.^{2,3}

A component that is being increasingly recognized as pivotal in the design of effective vaccines is the incorporation of appropriate immune potentiators (also termed adjuvants) along with the antigen. Adjuvants initiate early innate immune responses, which subsequently lead to the induction of robust and long-lasting adaptive immune responses.⁴ Aluminum salts (primarily phosphate and hydroxide), discovered by Glenny and co-workers,⁵ have been the only adjuvants in clinical use until the recent approval of 3-*O*-desacyl-4'-monophosphoryl lipid A (MPL) by the FDA.⁶ Aluminum salts are weak adjuvants for antibody induction, promoting a T helper 2 (Th2)-skewed, rather than a Th1, response;^{7,8} they are virtually ineffective at inducing cytotoxic T lymphocyte or mucosal immunoglobulin A (IgA) antibody responses, and they also appear to promote the induction of IgE isotype switching,

which has been associated with allergic reactions in some subjects.^{7,8}

Innate immune afferent signals activated by vaccine adjuvants include those originating from Toll-like receptors (TLRs) as well as retinoic acid-inducible gene 1 (RIG-I)-like receptors⁹ and nucleotide oligomerization domain (NOD)-like receptors (NLRs).^{10,11} There are 10 functional TLRs encoded in the human genome, which are transmembrane proteins with an extracellular domain having leucine-rich repeats (LRR) and a cytosolic domain called the Toll/IL-1 receptor (TIR) domain.¹² The ligands for these receptors are highly conserved molecules such as lipopolysaccharides (LPS) (recognized by TLR4), lipopeptides (TLR2 in combination with TLR1 or TLR6), flagellin (TLR5), single-stranded RNA (TLR7 and TLR8), double-stranded RNA (TLR3), CpG-motif-containing DNA (recognized by TLR9), and profilin present on uropathogenic bacteria (TLR11).¹² TLR1, -2, -4, -5, and -6 recognize extracellular stimuli, whereas TLR3, -7, -8, and -9 function within the endolysosomal compartment.¹² The activation of TLRs by their cognate ligands leads to the production of inflammatory cytokines and the upregulation of major histocompatibility complex (MHC) molecules and costimulatory signals in antigen-presenting cells (APCs) as well as activating natural killer (NK) cells (innate immune

Received: May 9, 2013

Published: July 30, 2013



response), which lead to the priming and amplification of T- and B-cell effector functions (adaptive immune responses).^{13–16}

We have recently embarked on a systematic exploration^{17,18} of a variety of TLR agonists with a view toward identifying safe and potent vaccine adjuvants. The chemotypes that we have explored thus far include agonists of TLR2,^{19–21} TLR7,^{22–26} TLR8,^{27,28} NOD1,²⁹ and C–C chemokine receptor type 1.³⁰

Our efforts are currently focused on evaluating small-molecule agonists of TLR8 as potential vaccine adjuvants. TLR8 is expressed in myeloid DCs, monocytes, and monocyte-derived dendritic cells, and the engagement of TLR8 agonists induces a dominant proinflammatory cytokine profile including tumor necrosis factor- α (TNF- α), interleukin-12 (IL-12), and IL-18.³¹ The prominent nuclear factor- κ B (NF- κ B)- and c-Jun N-terminal kinase (JNK)-mediated stimulatory effects of TLR8 agonists on APCs^{32,33} lead to robust Th1-type responses.³⁴ Unlike TLR2, -4, or -7 agonists, TLR8 agonists appear unique in their ability to markedly upregulate the production of the Th1-polarizing cytokines TNF- α and IL-12 from neonatal APCs,³⁴ suggesting that TLR8 agonists may be useful as adjuvants for enhancing immune responses in newborns.

Furthermore, human T-regulatory cells (Tregs), classified immunophenotypically as naturally occurring (CD4 $^{+}$ CD25 $^{+}$ Foxp3 $^{+}$) or induced (CD4 $^{+}$ CD25 high), downregulate and suppress a broad array of immune responses, including the nonspecific suppression of both CD4 $^{+}$ and CD8 $^{+}$ T-cells via cell–cell contact and production of immunosuppressive cytokines such as IL-10 and transforming growth factor- β (TGF- β).^{35–41} Tregs express abundant TLR8 mRNA, and TLR8 agonists have been shown to reverse Treg function via a TLR8–MyD88 (myeloid differentiation factor 88)–IRAK4 (IL-1-receptor-associated kinase 4) signaling pathway.⁴² The engagement and activation of TLR8 is, therefore, strongly associated with enhanced adaptive immune responses.

A prerequisite for the careful evaluation of TLR8 activators as potential adjuvants for neonatal vaccines is the availability of pure TLR8 agonists with negligible TLR7 activity and, other than the 2,3-diamino-furo[2,3-*c*]pyridine class of compounds recently described by us,²⁸ all other known agonists of TLR8, such as the imidazoquinolines (for instance, 1),^{25,43} thiazoloquinolines (CL075, 2),^{27,44–47} and a 2-aminobenzazepine derivative (VTX-2337, 3),⁴⁸ display mixed TLR7/TLR8 agonism, with the sole exception of VTX-294,⁴⁹ whose complete structure has not been reported. The structures of these mixed agonists are shown in Figure 1. The 2,3-diamino-furo[2,3-*c*]pyridines are atypical and noncanonical in that although they activate TLR8-dependent NF- κ B signaling, they are devoid of proinflammatory cytokine-inducing activities.²⁸

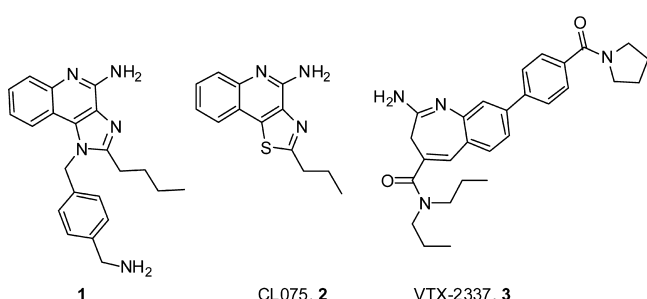


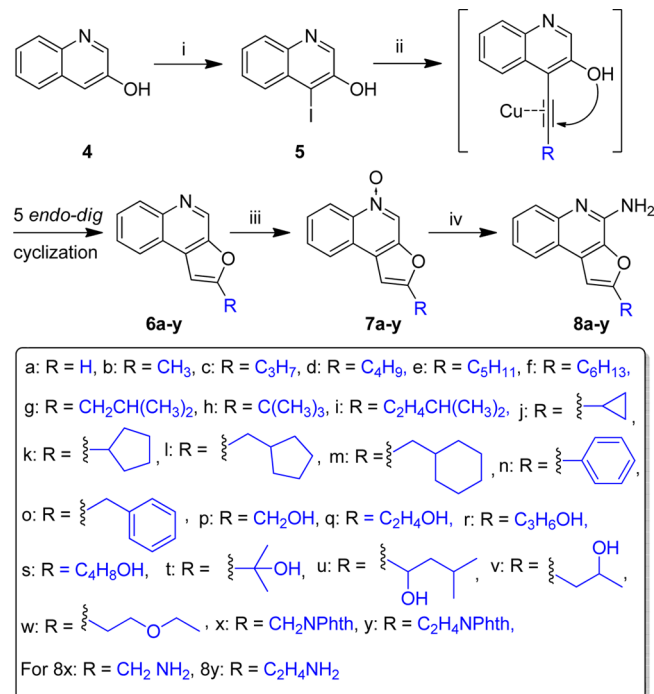
Figure 1. Representative TLR8/7 dual-agonistic heterocyclic small molecules.

Driven by our desire to identify pure TLR8 agonists also capable of inducing IL-12 and IL-18 and drawing from our earlier work in delineating structure–activity relationships (SAR) in the furo[2,3-*c*]pyridines, we began exploring a variety of fused heterocyclic core structures. Our continuing investigations have led to the discovery of pure TLR8-agonistic activity associated with strong interferon- γ (IFN- γ), IL-12-, and IL-18-inducing activities in a series of furo[2,3-*c*]quinolines. The 4-amino-furo[2,3-*c*]quinoline chemotype is unprecedented in the literature, and the activity profile of this class of compounds, examined by a range of secondary screens in human *ex vivo* blood models, including transcriptomal profiling, confirmed pure TLR8 agonism with no detectable signatures of TLR7 activity, allowing for the first time a clear path toward the evaluation of such compounds as potential adjuvants for vaccines.

■ RESULTS AND DISCUSSION

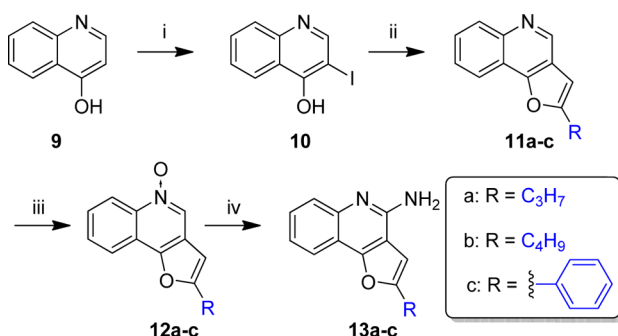
Our recent work on the 2,3-diamino-furo[2,3-*c*]pyridines, which display TLR8-dependent NF- κ B signaling but are dissociated from downstream cytokine induction, led us to consider benzologues of the furo[2,3-*c*]pyridines. The 4-amino-furo[2,3-*c*]quinoline chemotype is hitherto not described in the literature, and it presented a good starting point because its scaffold closely resembles known TLR7/8-active ligands. We envisioned that the furo[2,3-*c*]quinoline and its regioisomeric core structures could be derived via one-pot Sonogashira coupling of alkynes to either 4-iodoquinolin-3-ol (Scheme 1) or 3-iodoquinolin-4-ol (Scheme 2) followed by a tandem, tethered nucleophile-assisted, intramolecular 5-*endo*-dig cyclization.⁵⁰ Electrophilic iodination of commercially available 3- and 4-

Scheme 1. Syntheses of C2-Alkylfuro[2,3-*c*]quinoline Analogs^a



^aReagents: (i) I_2 , KI , NaOH ; (ii) $\text{Pd}(\text{PPh}_3)_4$, CuI , alkyne, $\text{Et}_3\text{N}/\text{CH}_3\text{CN}$ (1:3); (iii) *m*-CPBA, CHCl_3 ; and (iv) (a) benzoyl isocyanate, CH_2Cl_2 and (b) NaOCH_3 , MeOH .

Scheme 2. Syntheses of C2-alkylfuro[3,2-*c*]quinoline analogues^a



^aReagents: (i) I_2 , KI , $NaOH$; (ii) $Pd(PPh_3)_4$, CuI , alkyne, Et_3N/CH_3CN (1:3); (iii) $m\text{-}CPBA$, $CHCl_3$; and (iv) (a) benzoyl isocyanate, CH_2Cl_2 and (b) $NaOCH_3$, $MeOH$.

hydroxyquinoline proceeded uneventfully using reported methods (Schemes 1 and 2, respectively).⁵¹ One-pot Sonogashira coupling with a variety of alkynes followed by 5-endo-dig cyclization yielded compounds the 2-substituted furo[2,3-*c*]quinolines **6a**–**y** (Scheme 1) and the regioisomeric furo[3,2-*c*]quinolines **11a**–**c** (Scheme 2) in good yields. Target compounds **8a**–**y** and **13a**–**c** bearing 4-amino groups were obtained using conventional procedures described previously.^{23,27,44} Compounds **8a**–**y** and **13a**–**c** were screened in a panel of reporter-gene assays for human TLR2, -3, -4, -5, -7, -8, and -9 and NOD1, -2 modulatory activities. We were fortunate that a distinct activity profile was observed in the very first set of compounds that were synthesized. Compounds **8b**–**f** showed pure TLR8-agonistic activity, with maximal potency exhibited by **8d** with a C2-butyl group ($EC_{50} = 1.6 \mu M$, Figure 2); shorter (**8b**, **8c**) and longer (**8e**, **8f**) homologues displayed lower agonistic potencies, with shortest analogue **8a** being inactive (Figure 2). The dose–response profiles show characteristic biphasic responses (dose-dependent activation followed by the apparent suppression of NF- κ B translocation, Figure 2), as we had previously observed in several chemotypes.^{23,28,52} We verified that the apparent suppression was not due to cytotoxicity using LDH release and mitochondrial redox-based assays, as described earlier by us.^{53,54}

The SAR pattern with maximal activity conferred by a C2-butyl group is virtually identical to that found in TLR7-active imidazoquinolines²³ and the TLR8/7-agonistic thiazoloquinolines,²⁷ but unlike the thiazoloquinolines,²⁷ **8d** was devoid of TLR7-stimulatory activities in primary screens (Figure 2). The exquisite selectivity for TLR8 was confirmed in secondary screens using ex vivo whole human blood and PBMC models.¹⁷ We had earlier shown that proinflammatory cytokine induction (TNF- α , IL-1 β , IL-6, and IL-8) is a consequence of TLR8 activation.¹⁸ Importantly, Th1-biasing IL-12 and IL-18 induction is also TLR8-dependent, whereas IFN- α production is TLR7-mediated.^{24,52} Therefore, we examined the cytokine- and interferon-induction profiles of **8d**, employing thiazoloquinoline **2** as a reference compound. Unlike the 2,3-diamino-furo[2,3-*c*]pyridines,²⁸ **8d** was observed to induce TNF- α , IL-1 β , IL-6, and IL-8 in a dose-dependent manner, albeit with a lower potency than **2** (Figure 3). Compound **8d** induced IL-12 and IL-18 but was bereft of IFN- α -inducing properties (Figure 4). The selectivity of **8d** for TLR8 was also reflected in the absence of natural killer lymphocyte activation^{17,18} in human whole blood models, as assessed by cluster of differentiation 69

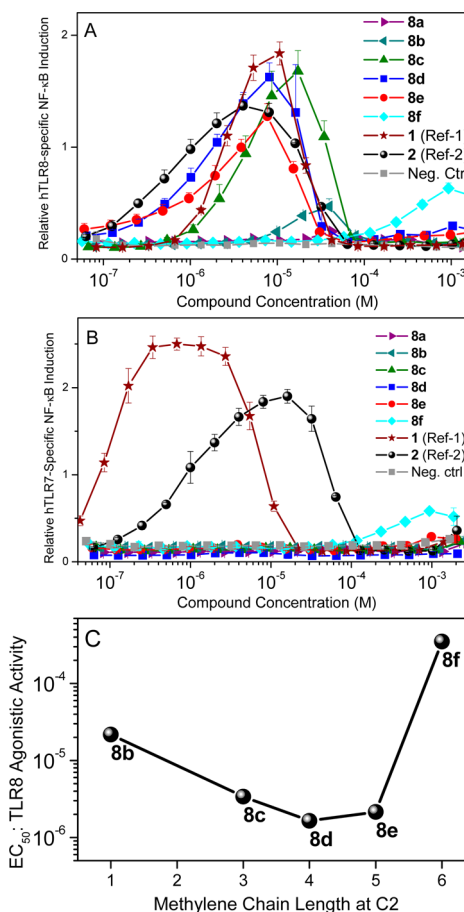


Figure 2. Dose–response profiles of human TLR8 (panel A) and human TLR7 (panel B) agonism by select C2-alkyl furo[2,3-*c*]quinolines. Error bars represent standard deviations obtained from quadruplicates. Dual TLR7/8-agonistic compounds **1** and **2** were used as comparators. Potency of TLR8 agonism (EC_{50} values) of a homologous series of C2-alkyl analogues (panel C). Compound **8a** was inactive.

(CD69) expression (Figure 5), which we had previously shown to be TLR7-dependent.^{17,18} Consistent with the above findings, transcriptomal profiling experiments showed strong induction of proinflammatory cytokine transcripts (including IL-12 and IL-18) by both **2** and **8d**, but IFN- α transcription was induced by only **2** owing to its dual TLR8/7-agonistic activity (Table 1). These data collectively confirm the selectivity of **8d** for human TLR8.

Given that **8d** represents an optimized compound in a uniquely TLR8-specific chemotype, we also profiled its cytokine- and chemokine-inducing properties using a 41-analyte multiplexed assay by comparing **8d** to a variety of TLR agonists. We found that of the 41 analytes analyzed both **8d** and **2** induced granulocyte colony-stimulating factor (G-CSF), growth-related oncogene (GRO), and macrophage inflammatory proteins 1- α and - β (MIP-1 α , MIP-1 β), whereas highly potent, pure TLR7-agonistic imidazoquinoline (1-benzyl-2-butyl-1*H*-imidazo[4,5-*c*]quinolin-4-amine) that we identified in our earlier SAR studies²³ did not (Figure 6), indicating that this set of analytes could be useful in distinguishing TLR8-specific responses.

Distinct hints that the SAR in the 2-substituted furo[2,3-*c*]quinolines was much more stringent compared to the thiazoloquinolines²⁷ were evident from the outset. C2

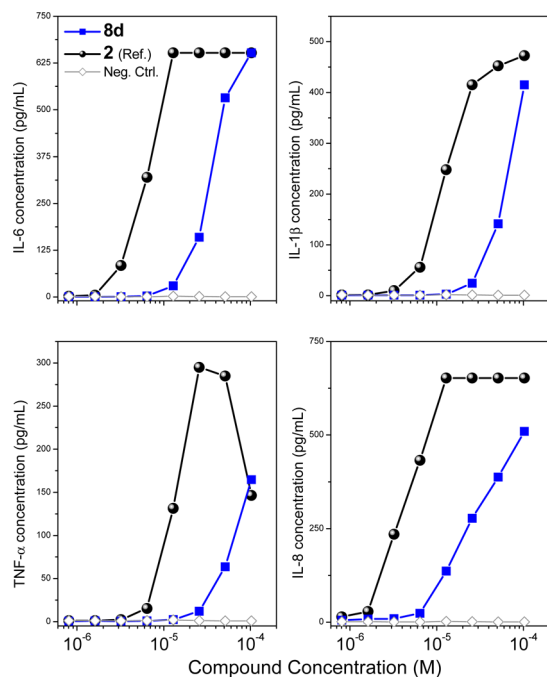


Figure 3. Proinflammatory cytokine induction profiles of **8d** in human blood. **2** was used as reference/comparator compound. The mean of duplicate values from a representative experiment is shown.

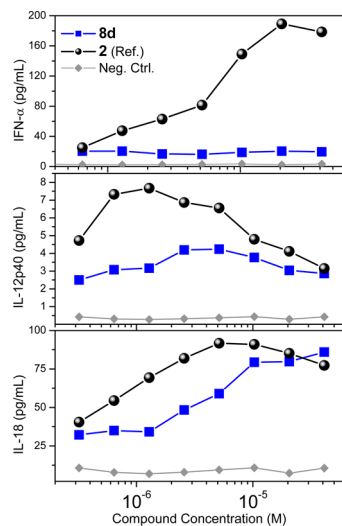


Figure 4. Dose-response profiles of IL-12p40 and IL-18 induction and the absence of IFN- α by **8d**. **2** was used as reference/comparator compound. The mean of duplicate values from a representative experiment is shown.

substituents with branched alkyl groups (**8g–i**) abrogated activity, and analogues with cycloaliphatic (**8j–8m**) or aromatic (**8n, 8o**) substituents were inactive, pointing to the intolerance of steric bulk at the putative binding site(s). Because the crystal structure of TLR8 was not available at the time, we forged on, surmising that the introduction of polar H-bond donors (or acceptors) on the C2 alkyl group may help us to understand better the binding-site interactions. Therefore, we examined a number of analogues bearing hydroxyl groups at various positions along the C2-alkyl chain (**8p–8v**), compounds with C2 substituents terminating with a primary amine (**8x, 8y**), and an analogue with an ether (H-bond acceptor) incorporated in

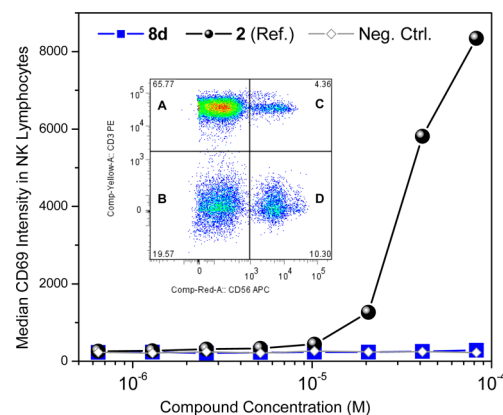


Figure 5. Absence of CD69 upregulation in human natural killer cells by **8d**. Flow cytometry data (inset) with gating on lymphocytes showing CD3 $^{+}$ CD56 $^{-}$ (T cells, quadrant A), CD3 $^{-}$ CD56 $^{-}$ (nominal B cells, quadrant B), CD3 $^{+}$ CD56 $^{+}$ (cytokine-induced killer cells, quadrant C), and CD3 $^{-}$ CD56 $^{+}$ (natural killer cells, quadrant D).

the alkyl group (**8w**), but none of these compounds were active in any of our primary screens.

Because we were mindful of our earlier observation that regioisomerism in the imidazoquinolines resulted in a switch from agonistic to antagonistic activities,^{22,55} we also synthesized key regioisomeric furo[3,2-*c*]quinolines **13a–c** (Scheme 2); these compounds were quiescent, displaying neither stimulatory nor inhibitory activity in primary screens. Given the fastidious structural requirements at the C2 position, we next synthesized a furo[2,3-*c*]isoquinoline with a C2-butyl substituent (**18**, Scheme 3) to explore the chemical space beyond the fused-quinoline chemotypes, but we were disappointed that **18** was also inactive.

Reverting, therefore, to the C2-butyl furo[2,3-*c*]quinoline, we interrogated the effect of introducing substituents at the C1 position. In particular, we desired to evaluate a C1-benzyl substituent because this strategy had previously yielded highly potent, TLR7-selective agonists in the imidazoquinoline series.²³ Electrophilic bromination of **7d** furnished precursor **19** in good yield (Scheme 4), which was carried forward to obtain both 1-bromo- and 1-benzyl-substituted analogues **21** and **24**, respectively (Scheme 4). Both analogues were found to be inactive.

As mentioned earlier, the 2,3-diamino-furo[2,3-*c*]pyridine class of compounds recently described by us²⁸ activate TLR8 but do not result in downstream cytokine production, suggesting an apparent dissociation between receptor occupancy and the signal-transduction events leading to cytokine production, and it was of interest to compare the SAR that we had gleaned from the furo[2,3-*c*]quinolines with select analogues of the 4-amino, C2-alkyl furo[2,3-*c*]pyridine series. Two such compounds (**28a, 28b**) were therefore synthesized (Scheme 5). Both of these analogues retained TLR8-selective agonistic activities but were substantially weaker ($EC_{50} = 24.4$ and $46.2 \mu M$, respectively) than **8d** ($EC_{50} = 1.6 \mu M$).

Although at first glance our attempts at exploring SAR in the furo[2,3-*c*]quinolines had yielded a large number of inactive compounds, we were delighted in no small measure that we have finally arrived at pure TLR8 agonists that induce the expected complement of TLR8-mediated, Th1-biasing cytokine mediators but are devoid of TLR7-dependent IFN- α -inducing properties. Just as we were concluding our studies on the furo[2,3-*c*]quinolines, crystal structures of hTLR8 complexed

Table 1. Transcriptomal Profiling of 8d in Human PBMCs

probeset ID	gene symbol	gene title	Log(FC) 2 vs neg. ctrl.	Log(FC) 8d vs neg. ctrl.
208375_at	IFNA1	interferon, alpha 1	7.38297	0.5418
208344_x_at	IFNA1 // IFNA13	interferon, alpha 1//13	5.36195	0.85859
208261_x_at	IFNA10	interferon, alpha 10	5.87577	0.7771
211405_x_at	IFNA17	interferon, alpha 17	4.25712	0.81187
211145_x_at	IFNA21	interferon, alpha 21	4.96822	0.58271
214569_at	IFNA5	interferon, alpha 5	7.03922	1.22985
208259_x_at	IFNA7	interferon, alpha 7	5.77059	0.80266
207932_at	IFNA8	interferon, alpha 8	4.18566	0.61895
210354_at	IFNG	interferon, gamma	5.60123	4.54852
204470_at	CXCL1	chemokine (C-X-C motif) ligand 1	0.88813	1.99629
209774_x_at	CXCL2	chemokine (C-X-C motif) ligand 2	2.83012	2.8543
207850_at	CXCL3	chemokine (C-X-C motif) ligand 3	1.47026	1.75638
215101_s_at	CXCL5	chemokine (C-X-C motif) ligand 5	1.51721	2.39582
203915_at	CXCL9	chemokine (C-X-C motif) ligand 9	1.88404	0.81365
204533_at	CXCL10	chemokine (C-X-C motif) ligand 10	7.689	6.42653
210163_at	CXCL11	chemokine (C-X-C motif) ligand 11	8.89003	6.50285
211122_s_at	CXCL11	chemokine (C-X-C motif) ligand 11	9.00636	6.56354
210118_s_at	IL1A	interleukin 1, alpha	4.67389	4.82369
205067_at	IL1B	interleukin 1, beta	2.45708	2.44858
216243_s_at	IL1RN	interleukin 1 receptor antagonist	3.97769	3.66761
207538_at	IL4	interleukin 4	2.20255	2.24232
205207_at	IL6	interleukin 6	7.85102	7.67767
207901_at	IL12B	interleukin 12B (natural killer cell stimulatory factor 2)	5.84181	3.26706
207844_at	IL13	interleukin 13	1.57695	2.04086
205992_s_at	IL15	interleukin 15	1.16516	1.06962
209827_s_at	IL16	interleukin 16	-1.7103	-0.64723
206295_at	IL18	interleukin 18	2.64035	2.40756
207072_at	IL18RAP	interleukin 18 receptor accessory protein	1.12674	0.51353
224071_at	IL20	interleukin 20	0.31683	0.81046
222974_at	IL22	interleukin 22	2.16422	0.38534
220054_at	IL23A	interleukin 23, alpha subunit p19	4.73191	4.96526
206569_at	IL24	interleukin 24	-0.6150	-0.00233
205926_at	IL27RA	interleukin 27 receptor, alpha	0.20872	0.16269
1552915_at	IL28A	interleukin 28A (interferon, lambda 2)	1.65564	0.59624
244261_at	IL28RA	interleukin 28 receptor, alpha (interferon, lambda receptor)	1.13284	0.78929
1552917_at	IL29	interleukin 29 (interferon, lambda 1)	1.02924	0.76252
203828_s_at	IL32	interleukin 32	0.35684	0.70521
207113_s_at	TNF	tumor necrosis factor	3.81754	3.3126
206025_s_at	TNFAIP6	tumor necrosis factor, alpha-induced protein 6	4.28297	4.17629

with mixed TLR7/TLR8-agonistic imidazoquinolines and thiazoloquinolines were reported,⁵⁶ allowing us to rationalize our experimentally determined SAR on the pure TLR8-agonistic furo[2,3-*c*]quinolines. The crystal structure of human TLR8 in complex with **2** (PDB ID: 3W3K)⁵⁶ was

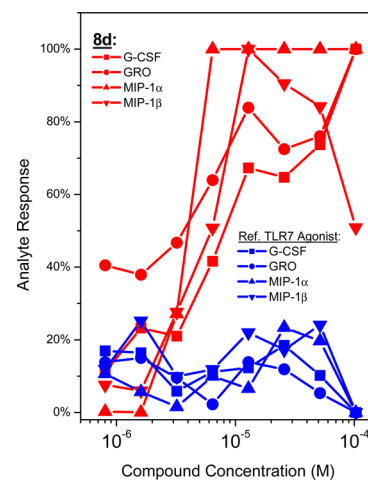
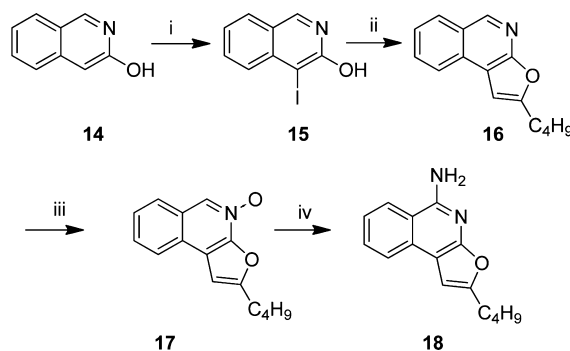


Figure 6. Disparate responses in select analytes (out of 41 analytes) in human PBMCs. G-CSF, GRO, MIP-1 α , and MIP-1 β are induced by **8d** (and **2**, data not shown) but not by a pure TLR7-agonistic imidazoquinoline. Dose responses represent the percent of the maximal response (G-CSF, 622 pg/mL; GRO, 515 pg/mL; MIP-1 α , 10 780 pg/mL; and MIP-1 β , 10 374 pg/mL). The mean of duplicate values from a representative experiment is shown. Analytes that were below the detection limits for the negative controls (medium alone) are not shown for clarity.

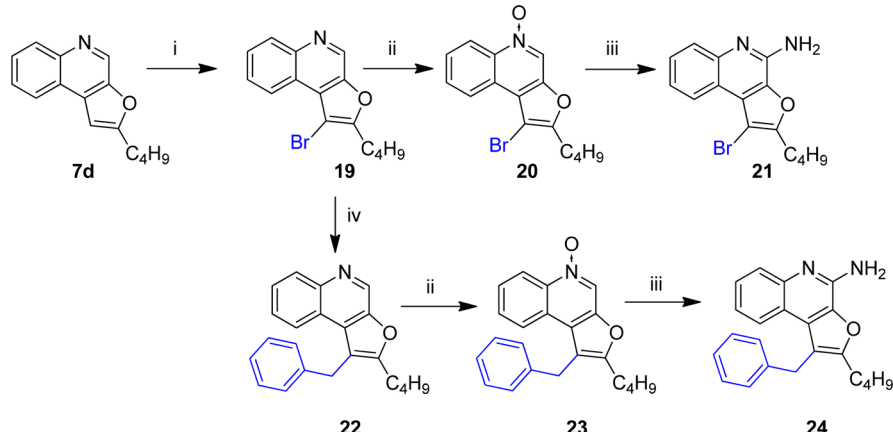
Scheme 3. Syntheses of C2-Alkylfuro[2,3-*c*]isoquinoline Analogues^a



^aReagents: (i) I_2 , KI, NaOH; (ii) $Pd(PPh_3)_4$, CuI, alkyne, Et_3N/CH_3CN (1:3); (iii) *m*-CPBA, $CHCl_3$; and (iv) (a) benzoyl isocyanate, CH_2Cl_2 and (b) $NaOCH_3$, $MeOH$.

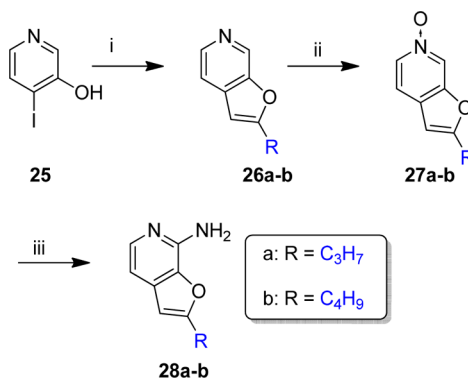
used for docking studies. We employed induced-fit methods^{57,58} in which the receptor sites were allowed conformational and torsional flexibility to simulate realistic ligand–receptor interactions to account for conformational changes in the binding site residues. Compounds **2** and **8d** occupy the same binding pocket formed by both of the TLR8 protomers (Figure 7A,B), with the binding geometry of these compounds and interacting residues being virtually identical (Figure 7C,D). Strong ionic H bonds (salt bridges) are observed between the C4 amine of both **2** and **8d** with Asp543 of protomer B, with additional stabilization derived from an H bond between Thr574 (protomer B) and either the N3 atom of the thiazole ring of **2** or the oxygen atom of the furanyl ring of **8d**. π – π interactions of the quinoline moiety of **2** and **8d** (Phe405/Tyr353) as well as hydrophobic interactions of the C2-alkyl group (Phe346/Ile403/Gly376) occur exclusively with residues in protomer A (Figure 7C,D). All of these interactions appear indispensable. The butyl group of **8d** allows for excellent

Scheme 4. Syntheses of C1-Substituted Furo[2,3-*c*]quinoline Analogues^a



^aReagents: (i) Br_2 , CH_2Cl_2 ; (ii) *m*-CPBA, CHCl_3 ; (iii) (a) benzoyl isocyanate, CH_2Cl_2 , (b) NaOCH_3 , MeOH ; and (iv) $\text{Pd}(\text{dpdpf})\text{Cl}_2$, 2-benzyl-4,4,5,5-tetramethyl-1,3,2-dioxaborolane, Cs_2CO_3 , 1,4-dioxane.

Scheme 5. Syntheses of C2-Alkylfuro[2,3-*c*]pyridine Analogues^a



^aReagents: (i) Pd(PPh₃)₄, CuI, alkyne, Et₃N/CH₃CN (1:3); (ii) *m*-CPBA, CHCl₃; and (iii) (a) benzoyl isocyanate, CH₂Cl₂ and (b) NaOCH₃, MeOH.

nonpolar and van der Waals contacts in the rather shallow hydrophobic cavity, and homologues with increasing C2-chain length (**8e–8f**) dock poorly because of kinked and sterically unfavorable conformations of the alkyl group. Analogues with cycloaliphatic (**8j–8m**) and aromatic substituents (**8n, 8o**) do not fit in the hydrophobic pocket at all, leading to unrealistic docked conformations (not shown). The cavity is lined entirely with the side chains of hydrophobic residues, explaining why even length-optimized analogues bearing polar groups at the C2 position, such as **8r, 8u**, and **8v**, do not display TLR8 agonism. The feeble activity of furopyridine compounds **28a** and **28b** imply significant contributions to the binding free energies by the π – π interactions of the quinoline moiety with Tyr353 and Phe405. The imposition of additional steric bulk at C1 (compound **24**) is not tolerated in the cleft bounded by Phe261 and Ser352 (Figure 7D). Not only is the pivotal ionic H bond between the C4 amine of regioisomeric furo[3,2-*c*]quinoline **13b** and Asp543 weakened (3.8 Å) but also the additional H bond between the oxygen atom of the furan ring and Thr574 is lost, forcing **13b** to bind to TLR8 in an inverted fashion, with the C2-alkyl group facing the entrance to the binding site (Figure 7E). Highly unfavorable H bonds are also

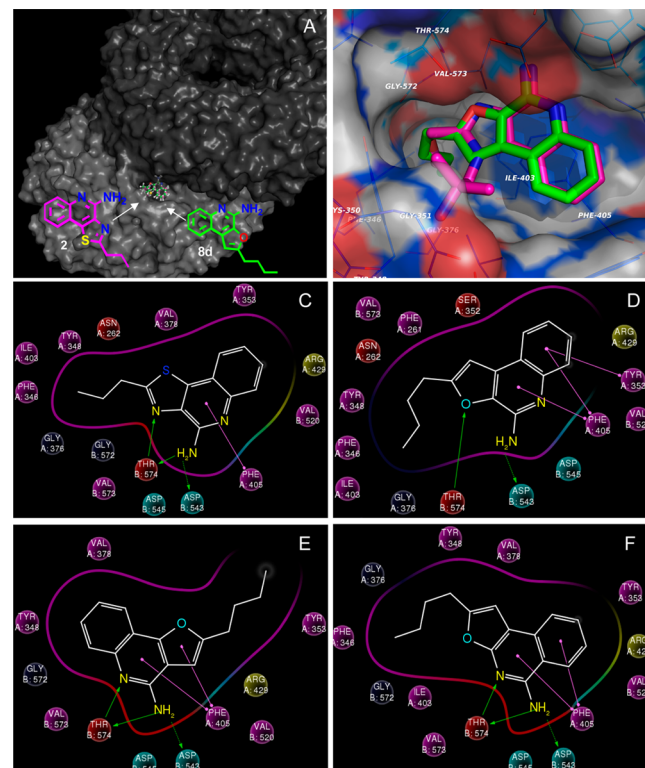


Figure 7. Induced-fit docking of ligands in human TLR8 (PDB ID: 3W3K). Both **2** and **8d** occupy the same binding pocket (panel A). Binding modes of the TLR7/8-dual active imidazoquinoline **CL097** and **8d** are superimposable (panel B). Binding-site interactions of **2**, **8d**, **13b**, and **18**, respectively (panels C–E).

seen in isoquinoline analogue **18**, especially with the loss of H-bonding of the furanyl oxygen (Figure 7F).

An exploration of furo[2,3-*c*]quinolines have yielded pure TLR8 agonists that are expected to possess strong Th1-biasing adjuvantic properties, as evidenced by prominent IL-12 and IL-18 induction profiles, and are without IFN- α -inducing properties, confirming their exquisite selectivity for human TLR8. The recently published atomic structure of human TLR8 has permitted a careful evaluation of SAR in this hitherto uncharacterized chemotype and provides clear directions

toward rational, structure-based ligand design. Immunization studies employing neonatal animal models are being planned with a view toward comparing the adjuvanticity of agonists with pure TLR7- and TLR8-agonistic properties vis-à-vis compounds with dual TLR7/8-stimulatory activities.

■ EXPERIMENTAL SECTION

Chemistry. All of the solvents and reagents used were obtained commercially and used as such unless noted otherwise. Moisture- or air-sensitive reactions were conducted under a nitrogen atmosphere in an oven-dried (120 °C) glass apparatus. The solvents were removed under reduced pressure using standard rotary evaporators. Flash column chromatography was carried out using RediSep Rf Gold high-performance silica columns on a CombiFlash Rf instrument unless otherwise mentioned, whereas thin-layer chromatography was carried out on silica gel (200 µm) CCM precoated aluminum sheets. The purity for all final compounds was confirmed to be greater than 97% by LC–MS using a Zorbax Eclipse Plus 4.6 mm × 150 mm, 5 µm analytical reverse-phase C18 column with H₂O–isopropanol or H₂O–CH₃CN gradients and an Agilent ESI-QTOF mass spectrometer (mass accuracy of 3 ppm) operating in the positive ion (or negative ion, as appropriate) acquisition mode.

Synthesis of 4-Iodoquinolin-3-ol (5). In an oven-dried round-bottomed flask equipped with a stirring bar was placed 3-hydroxy quinoline (1.0 g, 6.89 mmol) in 2N NaOH (20 mL). To this mixture, a solution of iodine (8.27 mmol) in 20% aqueous potassium iodide (20 mL) was added dropwise, and the mixture was stirred for 3 h at room temperature. The mixture was then acidified with acetic acid, and the precipitate was filtered and washed with water. After drying under vacuum, 1.50 g of 5 was obtained, which was used without purification. ^1H NMR (500 MHz, DMSO) δ 11.19 (s, 1H), 8.50 (s, 1H), 7.98–7.85 (m, 2H), 7.65–7.60 (m, 1H), 7.60–7.55 (m, 1H). ^{13}C NMR (126 MHz, DMSO) δ 152.2, 142.6, 141.3, 130.9, 129.9, 129.2, 128.5, 126.6, 94.5. MS (ESI) calcd for $\text{C}_9\text{H}_6\text{INO}$ (m/z), 270.95; found, 271.96 [$\text{M} + \text{H}]^+$.

General Procedure for the Sonogashira Reaction. To a stirred solution of 4-iodoquinolin-3-ol in acetonitrile/triethylamine (2:1) were added the appropriate alkyne (0.553 mmol), $\text{Pd}(\text{PPh}_3)_4$ (0.018 mmol), and CuI (0.018 mmol). The resulting reaction mixture was stirred at 70 °C under a nitrogen atmosphere for 12 h. After the completion of the reaction (monitored by TLC), the reaction mixture was diluted with water and extracted with ethylacetate (3 × 10 mL). The combined organic layer was dried over Na_2SO_4 and concentrated under reduced pressure, and the crude material was purified by flash chromatography using $\text{CH}_2\text{Cl}_2/\text{MeOH}$ as the eluent.

2-Propylfuro[2,3-*c*]quinoline (6c). Yellow solid (60 mg, 78%). ¹H NMR (500 MHz, CDCl₃) δ 9.08 (s, 1H), 8.20 (d, *J* = 8.2 Hz, 1H), 8.07 (dd, *J* = 8.1, 1.2 Hz, 1H), 7.67 (ddd, *J* = 8.4, 6.9, 1.5 Hz, 1H), 7.60 (ddd, *J* = 8.1, 7.0, 1.2 Hz, 1H), 6.91 (d, *J* = 0.8 Hz, 1H), 2.91–2.86 (m, 2H), 1.91–1.82 (m, 2H), 1.06 (t, *J* = 7.4 Hz, 3H). ¹³C NMR (126 MHz, CDCl₃) δ 163.0, 148.8, 144.3, 136.3, 131.4, 130.1, 127.3, 126.5, 123.7, 123.2, 101.1, 30.8, 21.2, 13.9. MS (ESI) calcd for C₁₄H₁₃NO (*m/z*), 211.10; found, 212.11 [M + H]⁺.

2-Butylfuro[2,3-*c*]quinoline (**6d**). Yellow solid (70 mg, 83%). ¹H NMR (500 MHz, CDCl₃) δ 9.08 (d, *J* = 0.5 Hz, 1H), 8.19 (dd, *J* = 8.4, 0.5 Hz, 1H), 8.09–8.05 (m, 1H), 7.66 (ddd, *J* = 8.4, 6.9, 1.5 Hz, 1H), 7.60 (ddd, *J* = 8.1, 7.0, 1.2 Hz, 1H), 6.90 (d, *J* = 0.8 Hz, 1H), 2.92 (t, 2H), 1.82 (ddd, *J* = 15.2, 8.5, 6.7 Hz, 2H), 1.51–1.42 (m, 2H), 0.99 (t, *J* = 7.4 Hz, 3H). ¹³C NMR (126 MHz, CDCl₃) δ 163.2, 148.8, 144.3, 136.4, 131.4, 130.1, 127.3, 126.5, 123.7, 123.2, 101.0, 29.9, 28.5, 22.4, 13.9. MS (ESI) calcd for C₁₅H₁₅NO (*m/z*), 225.11; found, 226.13 [M + H]⁺.

2-Pentylfuro[2,3-*c*]quinoline (6e). White solid (70 mg, 79%). ¹H NMR (500 MHz, CDCl₃) δ 9.08 (d, *J* = 0.7 Hz, 1H), 8.20 (dd, *J* = 8.4, 0.6 Hz, 1H), 8.07 (ddd, *J* = 8.1, 1.5, 0.6 Hz, 1H), 7.66 (ddd, *J* = 8.4, 6.9, 1.5 Hz, 1H), 7.60 (ddd, *J* = 8.1, 6.9, 1.3 Hz, 1H), 6.91–6.90 (m, 1H), 2.91 (t, *J* = 7.2 Hz, 2H), 1.88–1.80 (m, 2H), 1.46–1.35 (m, 4H), 0.93 (t, *J* = 7.1 Hz, 3H). ¹³C NMR (126 MHz, CDCl₃) δ 163.3, 148.8, 144.3, 136.4, 131.4, 130.1, 127.4, 126.5, 123.7, 123.2, 101.0, 31.5, 28.8,

27.5, 22.5, 14.1. MS (ESI) calcd for $C_{16}H_{17}NO$ (m/z), 239.13; found, 240.14 [$M + H$]⁺.

2-Hexylfuro[2,3-*c*]quinoline (6f). White solid (70 mg, 75%). ¹H NMR (500 MHz, CDCl₃) δ 9.08 (s, 1H), 8.20 (t, *J* = 8.3 Hz, 1H), 8.07 (dd, *J* = 8.1, 1.1 Hz, 1H), 7.66 (ddd, *J* = 8.4, 7.0, 1.5 Hz, 1H), 7.60 (ddd, 1H), 6.90 (d, *J* = 0.6 Hz, 1H), 2.91 (t, *J* = 7.6 Hz, 2H), 1.87–1.79 (m, 2H), 1.50–1.40 (m, 2H), 1.39–1.28 (m, 4H), 0.90 (t, *J* = 8.2, 5.9 Hz, 3H). ¹³C NMR (126 MHz, CDCl₃) δ 163.2, 148.8, 144.3, 136.3, 131.4, 130.1, 127.3, 126.5, 123.7, 123.2, 101.0, 31.7, 29.0, 28.9, 27.8, 22.7, 14.2. MS (ESI) calcd for C₁₇H₁₉NO (*m/z*), 253.15; found, 254.16 [M + H]⁺.

2-Isobutylfuro[2,3-*c*]quinoline (6g). Liquid (120 mg, 72%). ¹H NMR (500 MHz, CDCl₃) δ 9.12 (s, 1H), 8.25 (d, *J* = 8.2 Hz, 1H), 8.08 (d, *J* = 7.9 Hz, 1H), 7.69–7.64 (m, 1H), 7.63–7.58 (m, 1H), 6.91 (s, 1H), 2.79 (dd, *J* = 7.1, 0.5 Hz, 2H), 2.20 (dp, *J* = 13.6, 6.8 Hz, 1H), 1.03 (d, *J* = 6.7 Hz, 6H). ¹³C NMR (126 MHz, CDCl₃) δ 162.4, 144.3, 136.4, 131.5, 130.2, 127.4, 126.6, 123.7, 102.0, 38.0, 28.1, 22.6. MS (ESI) calcd for C₁₅H₁₅NO (*m/z*), 225.12; found, 226.13 [M + H]⁺.

2-(tert-Butyl)furo[2,3-*c*]quinoline (6h). White solid (69 mg, 83%).
 ^1H NMR (500 MHz, CDCl_3) δ 9.11 (s, 1H), 8.20 (d, J = 8.3 Hz, 1H), 8.08 (d, J = 7.9 Hz, 1H), 7.69–7.64 (m, 1H), 7.59 (t, J = 7.4 Hz, 1H), 6.89 (s, 1H), 1.47 (s, 9H). ^{13}C NMR (126 MHz, CDCl_3) δ 170.7, 148.8, 144.3, 136.4, 131.2, 130.1, 127.3, 126.5, 123.6, 123.4, 98.2, 33.6, 29.1. MS (ESI) calcd for $\text{C}_{15}\text{H}_{15}\text{NO}$ (m/z), 225.12; found, 226.14 [$\text{M} + \text{H}]^+$.

2-Isopentylfuro[2,3-c]quinoline (6i). Solid (65 mg, 74%). ¹H NMR (500 MHz, CDCl₃) δ 9.10 (s, 1H), 8.21 (d, *J* = 8.3 Hz, 1H), 8.07 (d, *J* = 7.9 Hz, 1H), 7.70–7.63 (m, 1H), 7.59 (t, 1H), 6.90 (s, 1H), 2.91 (t, 2H), 1.79–1.64 (m, 3H), 0.99 (d, *J* = 6.4 Hz, 6H). ¹³C NMR (126 MHz, CDCl₃) δ 163.4, 148.8, 144.3, 136.3, 131.4, 130.2, 127.3, 126.5, 123.7, 123.2, 100.9, 36.7, 27.8, 26.8, 22.5. MS (ESI) calcd for C₁₆H₁₇NO (*m/z*), 239.13; found, 240.14 [M + H]⁺.

2-Cyclopropylfuro[2,3-*c*]quinoline (6j). Solid (60 mg, 78%). ^1H NMR (500 MHz, CDCl_3) δ 9.02 (d, $J = 0.7$ Hz, 1H), 8.17 (dd, $J = 8.4, 0.6$ Hz, 1H), 8.04 (ddd, $J = 8.1, 1.5, 0.6$ Hz, 1H), 7.66 (ddd, $J = 8.4, 6.9, 1.5$ Hz, 1H), 7.58 (ddd, $J = 8.1, 6.9, 1.2$ Hz, 1H), 6.89–6.85 (m, 1H), 2.21–2.14 (m, 1H), 1.12 (dq, $J = 6.0, 2.4, 1.2$ Hz, 4H). ^{13}C NMR (126 MHz, CDCl_3) δ 164.0, 148.3, 144.4, 136.0, 131.7, 130.1, 127.4, 126.4, 123.7, 123.0, 99.4, 10.1, 8.5. MS (ESI) calcd for $\text{C}_{14}\text{H}_{11}\text{NO}$ (m/z), 209.10; found, 210.10 [M + H] $^+$.

2-Cyclopentylfuro[2,3-*c*]quinoline (6k). White solid (72 mg, 82%). ^1H NMR (500 MHz, CDCl_3) δ 9.08 (s, 1H), 8.20 (d, J = 8.3 Hz, 1H), 8.07 (d, J = 7.7 Hz, 1H), 7.70–7.64 (m, 1H), 7.59 (t, J = 11.0, 3.8 Hz, 1H), 6.91 (s, 1H), 3.41–3.31 (m, 1H), 2.23–2.13 (m, 2H), 1.95–1.81 (m, 4H), 1.81–1.69 (m, 2H). ^{13}C NMR (126 MHz, CDCl_3) δ 166.8, 144.3, 136.4, 131.3, 130.1, 127.3, 126.5, 123.7, 123.2, 99.6, 39.4, 32.1, 25.6. MS (ESI) calcd for $\text{C}_{16}\text{H}_{15}\text{NO}$ (m/z), 237.11; found, 238.13 [$\text{M} + \text{H}]^+$.

2-(Cyclopentylmethyl)furo[2,3-*c*]quinoline (6l). Solid (71 mg, 75%). ^1H NMR (500 MHz, CDCl_3) δ 9.10 (s, 1H), 8.22 (d, J = 8.2 Hz, 1H), 8.08 (d, J = 7.9 Hz, 1H), 7.67 (t, J = 7.0 Hz, 1H), 7.60 (t, 1H), 6.91 (s, 1H), 2.91 (d, J = 7.4 Hz, 2H), 2.38 (dt, J = 15.4, 7.8 Hz, 1H), 1.87 (m, 2H), 1.74–1.65 (m, 2H), 1.64–1.57 (m, 2H), 1.32 (m, 2H). ^{13}C NMR (126 MHz, CDCl_3) δ 163.0, 144.3, 136.4, 131.5, 130.2, 127.4, 126.5, 123.7, 101.5, 38.9, 34.9, 32.7, 25.2. MS (ESI) calcd for $\text{C}_{17}\text{H}_{17}\text{NO}$ (m/z), 251.13; found, 252.14 [$\text{M} + \text{H}]^+$.

2-(Cyclohexylmethyl)furo[2,3-*c*]quinoline (6m). Solid (170 mg, 87%). ¹H NMR (500 MHz, CDCl₃) δ 9.10 (s, 1H), 8.21 (d, *J* = 8.3 Hz, 1H), 8.07 (d, *J* = 7.7 Hz, 1H), 7.72–7.63 (m, 1H), 7.59 (t, *J* = 7.4 Hz, 1H), 6.89 (s, 1H), 2.78 (d, *J* = 6.9 Hz, 2H), 1.89–1.64 (m, 6H), 1.33–1.12 (m, 3H), 1.05 (qd, *J* = 12.4, 3.1 Hz, 2H). ¹³C NMR (126 MHz, CDCl₃) δ 162.1, 148.8, 144.23, 136.4, 131.4, 130.1, 127.3, 126.5, 123.7, 123.2, 102.0, 37.3, 36.7, 33.3, 26.4, 26.2. MS (ESI) calcd for C₁₈H₁₉NO (*m/z*), 265.15; found, 266.16 [M + H]⁺.

2-Phenylfuro[2,3-*c*]quinoline (6n). White solid (65 mg, 72%). ¹H NMR (500 MHz, CDCl₃) δ 9.20 (d, 1H), 8.23 (dd, *J* = 8.3, 0.7 Hz, 1H), 8.17 (ddd, *J* = 8.0, 1.5, 0.5 Hz, 1H), 8.01–7.97 (m, 2H), 7.71 (ddd, *J* = 8.4, 6.9, 1.6 Hz, 1H), 7.65 (ddd, *J* = 8.1, 7.0, 1.3 Hz, 1H), 7.55–7.50 (m, 3H), 7.47–7.43 (m, 1H). ¹³C NMR (126 MHz, CDCl₃) δ 158.8, 148.9, 144.5, 136.7, 131.6, 130.3, 129.8, 129.8, 129.2,

127.7, 126.9, 125.6, 123.7, 123.2, 99.9. MS (ESI) calcd for $C_{17}H_{11}NO$ (*m/z*), 245.10; found, 246.10 [M + H]⁺.

Furo[2,3-*c*]quinolin-2-ylmethanol (6p). Solid (56 mg, 77%). ¹H NMR (500 MHz, MeOD) δ 9.07 (s, 1H), 8.26 (dd, *J* = 8.0, 1.2 Hz, 1H), 8.12 (d, *J* = 8.2 Hz, 1H), 7.77–7.71 (m, 1H), 7.71–7.66 (m, 1H), 7.39 (s, 1H), 4.84 (s, 2H). ¹³C NMR (126 MHz, MeOD) δ 163.5, 150.2, 144.8, 137.2, 133.0, 129.7, 129.1, 128.3, 125.0, 124.6, 103.3, 58.1. MS (ESI) calcd for $C_{12}H_9NO_2$ (*m/z*), 199.10; found, 200.07 [M + H]⁺.

2-(Furo[2,3-*c*]quinolin-2-yl)ethanol (6q). Solid (58 mg, 74%). ¹H NMR (500 MHz, MeOD) δ 9.02 (s, 1H), 8.23 (dd, 1H), 8.10 (dd, *J* = 8.3, 0.5 Hz, 1H), 7.71 (ddd, *J* = 8.5, 7.0, 1.6 Hz, 1H), 7.67 (ddd, *J* = 8.1, 7.0, 1.3 Hz, 1H), 7.26 (d, *J* = 0.7 Hz, 1H), 4.01 (t, *J* = 6.4 Hz, 2H), 3.17 (td, *J* = 6.4, 0.6 Hz, 2H). ¹³C NMR (126 MHz, MeOD) δ 162.9, 149.9, 144.7, 136.7, 133.6, 129.6, 128.9, 128.0, 125.1, 124.4, 103.5, 60.6, 33.1. MS (ESI) calcd for $C_{13}H_{11}NO_2$ (*m/z*), 213.08; found, 214.09 [M + H]⁺.

4-(Furo[2,3-*c*]quinolin-2-yl)butan-1-ol (6s). Solid (68 mg, 77%). ¹H NMR (500 MHz, MeOD) δ 8.99 (s, 1H), 8.22–8.18 (m, 1H), 8.09 (dd, *J* = 8.4, 0.6 Hz, 1H), 7.70 (ddd, *J* = 8.4, 6.9, 1.6 Hz, 1H), 7.65 (ddd, *J* = 8.1, 7.0, 1.3 Hz, 1H), 7.17 (d, *J* = 0.8 Hz, 1H), 3.63 (t, *J* = 6.4 Hz, 2H), 2.98 (t, 2H), 1.96–1.88 (m, 2H), 1.71–1.63 (m, 2H). ¹³C NMR (126 MHz, MeOD) δ 165.5, 149.8, 144.7, 136.6, 133.6, 129.5, 128.9, 128.0, 125.1, 124.3, 102.4, 62.4, 33.0, 29.2, 25.2. MS (ESI) calcd for $C_{15}H_{15}NO_2$ (*m/z*), 241.11; found, 242.12 [M + H]⁺.

2-(Furo[2,3-*c*]quinolin-2-yl)propan-2-ol (6t). White solid (60 mg, 72%). ¹H NMR (500 MHz, MeOD) δ 9.07 (d, *J* = 0.6 Hz, 1H), 8.29–8.24 (m, 1H), 8.14–8.10 (m, 1H), 7.73 (ddd, *J* = 8.5, 7.0, 1.6 Hz, 1H), 7.68 (ddd, *J* = 8.1, 7.0, 1.3 Hz, 1H), 7.36 (d, *J* = 0.8 Hz, 1H), 1.72 (s, 6H). ¹³C NMR (126 MHz, MeOD) δ 169.7, 149.9, 144.8, 137.1, 133.0, 129.7, 129.0, 128.2, 125.0, 124.6, 100.6, 70.1, 29.1. MS (ESI) calcd for $C_{14}H_{13}NO_2$ (*m/z*), 227.10; found, 228.11 [M + H]⁺.

1-(Furo[2,3-*c*]quinolin-2-yl)propan-2-ol (6v). White solid (70 mg, 84%). ¹H NMR (500 MHz, MeOD) δ 9.04 (d, *J* = 0.5 Hz, 1H), 8.27–8.23 (m, 1H), 8.11 (dd, *J* = 8.4, 0.6 Hz, 1H), 7.73 (ddd, *J* = 8.5, 7.0, 1.6 Hz, 1H), 7.68 (ddd, *J* = 8.1, 7.0, 1.3 Hz, 1H), 7.28 (d, *J* = 0.7 Hz, 1H), 4.32–4.25 (m, 1H), 3.09 (d, *J* = 6.2 Hz, 2H), 1.31 (d, *J* = 6.2 Hz, 3H). ¹³C NMR (126 MHz, MeOD) δ 163.0, 149.9, 144.6, 136.7, 133.7, 129.5, 129.0, 128.1, 125.1, 124.4, 104.0, 67.1, 39.2, 23.4. MS (ESI) calcd for $C_{14}H_{13}NO_2$ (*m/z*), 227.10; found, 228.11 [M + H]⁺.

2-(2-Ethoxyethyl)furo[2,3-*c*]quinoline (6w). Solid (70 mg, 77%). ¹H NMR (500 MHz, CDCl₃) δ 9.10 (s, 1H), 8.21 (d, *J* = 8.3 Hz, 1H), 8.08 (dd, *J* = 8.1, 1.1 Hz, 1H), 7.68 (ddd, *J* = 8.4, 7.0, 1.4 Hz, 1H), 7.63–7.59 (m, 1H), 7.02 (d, 1H), 3.87 (t, *J* = 6.6 Hz, 2H), 3.57 (q, *J* = 7.0 Hz, 2H), 3.20 (td, *J* = 6.6, 0.8 Hz, 2H), 1.23 (t, *J* = 7.0 Hz, 3H). ¹³C NMR (126 MHz, CDCl₃) δ 160.1, 148.8, 144.3, 136.3, 131.4, 130.1, 127.3, 126.6, 123.7, 123.2, 102.3, 68.0, 66.7, 29.8, 15.3. MS (ESI) calcd for $C_{15}H_{15}NO_2$ (*m/z*), 241.11; found, 242.11 [M + H]⁺.

2-(Furo[2,3-*c*]quinolin-2-ylmethyl)isoindoline-1,3-dione (6x). White solid (33 mg, 61%). ¹H NMR (500 MHz, DMSO) δ 9.20 (d, *J* = 0.5 Hz, 1H), 8.32 (d, 1H), 8.11 (dd, *J* = 8.3, 0.7 Hz, 1H), 7.96 (dd, *J* = 5.5, 3.0 Hz, 2H), 7.89 (dd, *J* = 5.5, 3.1 Hz, 2H), 7.75–7.64 (m, 3H), 5.11 (d, *J* = 0.4 Hz, 2H). ¹³C NMR (126 MHz, DMSO) δ 167.3, 155.6, 148.3, 143.7, 136.6, 134.8, 131.6, 130.1, 129.6, 127.7, 126.9, 124.1, 123.5, 122.6, 103.8, 34.9. MS (ESI) calcd for $C_{20}H_{12}N_2O_3$ (*m/z*), 328.08; found, 329.10 [M + H]⁺.

2-(2-(Furo[2,3-*c*]quinolin-2-yl)ethyl)isoindoline-1,3-dione (6y). White solid (65 mg, 77%). ¹H NMR (500 MHz, DMSO) δ 9.13 (s, 1H), 8.23 (dd, *J* = 8.0, 1.4 Hz, 1H), 8.10 (d, *J* = 8.2 Hz, 1H), 7.90–7.79 (m, 4H), 7.73–7.68 (m, 1H), 7.68–7.63 (m, 1H), 7.44 (s, 1H), 4.03 (t, *J* = 6.9 Hz, 2H), 3.30 (t, *J* = 6.9 Hz, 2H). ¹³C NMR (126 MHz, DMSO) δ 167.7, 158.9, 148.5, 143.7, 136.2, 134.5, 131.6, 130.4, 129.5, 127.5, 126.7, 124.0, 123.2, 122.6, 103.1, 36.0, 27.3. MS (ESI) calcd for $C_{21}H_{14}N_2O_3$ (*m/z*), 342.10; found, 343.12 [M + H]⁺.

General Procedure for N-Oxidation. To a stirred solution of substrate (0.53 mmol) in CHCl₃ was added *m*-CPBA (1.06 mmol). The resulting reaction mixture was stirred at room temperature for 4 h. After the completion of the reaction (monitored by TLC), the reaction mixture was diluted with water and extracted with CH₂Cl₂ (3 \times 10

mL). The combined organic layer was dried over Na₂SO₄ and concentrated under reduced pressure, and the crude material was purified by flash chromatography.

2-Methylfuro[2,3-*c*]quinoline 5-oxide (7b). White solid (80 mg, 74%). ¹H NMR (500 MHz, CDCl₃) δ 8.86 (s, 1H), 8.84 (dd, 1H), 8.08–8.03 (m, 1H), 7.76–7.68 (m, 2H), 6.87 (t, 1H), 2.59 (d, *J* = 1.0 Hz, 3H). ¹³C NMR (126 MHz, CDCl₃) δ 159.7, 147.2, 138.8, 129.0, 128.6, 124.5, 124.3, 122.7, 121.0, 102.2, 14.5. MS (ESI) calcd for $C_{12}H_9NO_2$ (*m/z*), 199.10; found, 200.06 [M + H]⁺.

2-Propylfuro[2,3-*c*]quinoline 5-oxide (7c). White solid (78 mg, 72%). ¹H NMR (500 MHz, CDCl₃) δ 8.88–8.82 (m, 2H), 8.08–8.04 (m, 1H), 7.75–7.68 (m, 2H), 6.86 (dd, *J* = 1.7, 0.8 Hz, 1H), 2.88–2.83 (m, 2H), 1.88–1.79 (m, 2H), 1.05 (t, *J* = 7.4 Hz, 3H). ¹³C NMR (126 MHz, CDCl₃) δ 163.7, 147.1, 138.8, 128.9, 128.5, 124.4, 124.2, 124.1, 122.8, 121.1, 101.4, 30.7, 21.1, 13.9. MS (ESI) calcd for $C_{14}H_{13}NO_2$ (*m/z*), 227.10; found, 228.10 [M + H]⁺.

2-Butylfuro[2,3-*c*]quinoline 5-Oxide (7d). White solid (75 mg, 70%). ¹H NMR (500 MHz, CDCl₃) δ 8.86 (d, *J* = 0.5 Hz, 1H), 8.85–8.83 (m, 1H), 8.08–8.04 (m, 1H), 7.75–7.68 (m, 2H), 6.86 (d, *J* = 0.9 Hz, 1H), 2.90–2.86 (m, 2H), 1.82–1.76 (m, 2H), 1.46 (dq, *J* = 14.7, 7.4 Hz, 2H), 0.98 (t, *J* = 7.4 Hz, 3H). ¹³C NMR (126 MHz, CDCl₃) δ 164.0, 147.1, 138.7, 128.9, 128.5, 124.5, 124.2, 124.2, 122.8, 121.0, 101.3, 29.8, 28.5, 22.4, 13.9. MS (ESI) calcd for $C_{15}H_{15}NO_2$ (*m/z*), 241.11; found, 242.12 [M + H]⁺.

2-Pentylfuro[2,3-*c*]quinoline 5-Oxide (7e). White solid (77 mg, 72%). ¹H NMR (500 MHz, CDCl₃) δ 8.87–8.86 (m, 1H), 8.86–8.83 (m, 1H), 8.09–8.05 (m, 1H), 7.76–7.68 (m, 2H), 6.86 (d, *J* = 0.8 Hz, 1H), 2.87 (t, *J* = 7.4 Hz, 2H), 1.84–1.78 (m, 2H), 1.40 (qd, *J* = 4.6, 1.7 Hz, 2H), 0.93 (t, *J* = 7.1 Hz, 3H). ¹³C NMR (126 MHz, CDCl₃) δ 164.0, 147.1, 138.7, 128.9, 128.5, 124.5, 124.2, 124.2, 122.8, 121.1, 101.3, 31.5, 28.8, 27.4, 22.5, 14.1. MS (ESI) calcd for $C_{16}H_{17}NO_2$ (*m/z*), 255.12; found, 256.14 [M + H]⁺.

2-Hexylfuro[2,3-*c*]quinoline 5-Oxide (7f). White solid (105 mg, 82%). ¹H NMR (500 MHz, CDCl₃) δ 8.86 (d, *J* = 0.5 Hz, 1H), 8.86–8.82 (m, 1H), 8.08–8.05 (m, 1H), 7.75–7.68 (m, 2H), 6.86 (d, *J* = 0.9 Hz, 1H), 2.87 (t, *J* = 7.3 Hz, 2H), 1.80 (dt, *J* = 15.2, 7.5 Hz, 2H), 1.47–1.39 (m, 2H), 1.36–1.30 (m, 4H), 0.90 (t, *J* = 7.1 Hz, 3H). ¹³C NMR (126 MHz, CDCl₃) δ 164.0, 147.1, 138.8, 128.9, 128.5, 124.5, 124.2, 124.2, 122.8, 121.1, 101.3, 31.6, 29.0, 28.8, 27.7, 22.7, 14.2. MS (ESI) calcd for $C_{17}H_{19}NO_2$ (*m/z*), 269.14; found, 270.15 [M + H]⁺.

2-Isobutylfuro[2,3-*c*]quinoline 5-Oxide (7g). Solid (100 mg, 78%). ¹H NMR (500 MHz, CDCl₃) δ 8.87 (s, 1H), 8.85 (dt, *J* = 7.2, 3.9 Hz, 1H), 8.09–8.06 (m, 1H), 7.76–7.69 (m, 2H), 6.88 (d, *J* = 0.7 Hz, 1H), 2.76 (dd, *J* = 7.1, 0.5 Hz, 2H), 2.22–2.12 (m, 1H), 1.03 (d, *J* = 6.7 Hz, 6H). ¹³C NMR (126 MHz, CDCl₃) δ 163.0, 147.2, 138.8, 128.9, 128.5, 124.5, 124.3, 124.1, 122.8, 121.1, 101.3, 31.6, 29.0, 28.8, 27.7, 22.7, 14.2. MS (ESI) calcd for $C_{15}H_{15}NO_2$ (*m/z*), 241.11; found, 242.13 [M + H]⁺.

2-(*tert*-Butyl)furo[2,3-*c*]quinoline 5-Oxide (7h). White solid (72 mg, 68%). ¹H NMR (500 MHz, CDCl₃) δ 8.88 (d, *J* = 0.6 Hz, 1H), 8.85 (dd, *J* = 7.8, 2.1 Hz, 1H), 8.09–8.06 (m, 1H), 7.75–7.69 (m, 2H), 6.85 (d, *J* = 0.9 Hz, 1H), 1.45 (s, 9H). ¹³C NMR (126 MHz, CDCl₃) δ 171.5, 147.1, 138.7, 128.9, 128.5, 124.6, 124.2, 124.1, 123.0, 121.1, 98.6, 29.0. MS (ESI) calcd for $C_{15}H_{15}NO_2$ (*m/z*), 241.11; found, 242.12 [M + H]⁺.

2-Isopentylfuro[2,3-*c*]quinoline 5-Oxide (7i). Solid (60 mg, 77%). ¹H NMR (500 MHz, MeOD) δ 9.13 (d, *J* = 0.5 Hz, 1H), 8.72 (dd, *J* = 8.1, 1.6 Hz, 1H), 8.37–8.34 (m, 1H), 7.90–7.83 (m, 2H), 7.28 (d, *J* = 0.8 Hz, 1H), 3.01–2.96 (m, 2H), 1.78–1.72 (m, 2H), 1.72–1.65 (m, 1H), 1.01 (d, *J* = 6.5 Hz, 6H). ¹³C NMR (126 MHz, MeOD) δ 167.7, 147.9, 138.8, 130.6, 130.5, 128.7, 126.7, 126.0, 124.0, 120.8, 102.8, 37.6, 28.9, 27.5, 22.7. MS (ESI) calcd for $C_{16}H_{17}NO_2$ (*m/z*), 255.12; found, 256.13 [M + H]⁺.

2-Cyclopropylfuro[2,3-*c*]quinoline 5-Oxide (7j). Solid (40 mg, 74%). ¹H NMR (500 MHz, MeOD) δ 9.11–8.99 (m, 1H), 8.73 (t, *J* = 13.1 Hz, 1H), 8.36–8.30 (m, 1H), 7.96–7.78 (m, 2H), 7.24 (s, 1H), 2.35–2.24 (m, 1H), 1.27–1.16 (m, 2H), 1.15–1.09 (m, 2H). ¹³C NMR (126 MHz, MeOD) δ 168.84, 130.7, 130.3, 129.8, 129.3, 126.0, 125.1, 123.6, 120.7, 100.9, 10.6, 9.2. MS (ESI) calcd for $C_{14}H_{11}NO_2$ (*m/z*), 225.10; found, 226.09 [M + H]⁺.

2-Cyclopentylfuro[2,3-*c*]quinoline 5-Oxide (7k). White solid (77 mg, 72%). ^1H NMR (500 MHz, MeOD) δ 9.12 (d, J = 0.4 Hz, 1H), 8.71 (dd, 1H), 8.35 (dd, 1H), 7.89–7.81 (m, 2H), 7.29 (d, J = 0.7 Hz, 1H), 3.47–3.39 (m, 1H), 2.26–2.14 (m, 2H), 1.96–1.85 (m, 4H), 1.81–1.72 (m, 2H). ^{13}C NMR (126 MHz, MeOD) δ 171.0, 147.9, 138.8, 130.6, 130.5, 128.7, 126.7, 126.0, 124.0, 120.8, 101.5, 40.5, 32.8, 26.4. MS (ESI) calcd for $\text{C}_{16}\text{H}_{15}\text{NO}_2$ (m/z), 253.11; found, 254.12 [M + H]⁺.

2-(Cyclopentylmethyl)furo[2,3-*c*]quinoline 5-Oxide (7l). White solid (75 mg, 70%). ^1H NMR (500 MHz, MeOD) δ 9.13 (s, 1H), 8.74–8.70 (m, 1H), 8.36 (dd, J = 7.5, 1.8 Hz, 1H), 7.91–7.82 (m, 2H), 7.29 (d, J = 0.5 Hz, 1H), 2.96 (d, J = 7.4 Hz, 2H), 2.44–2.37 (m, 1H), 1.93–1.85 (m, 2H), 1.75–1.67 (m, 2H), 1.65–1.58 (m, 2H), 1.40–1.32 (m, 2H). ^{13}C NMR (126 MHz, MeOD) δ 167.2, 147.9, 138.8, 130.6, 130.5, 128.7, 126.7, 126.0, 124.0, 120.8, 103.3, 40.0, 35.5, 33.5, 26.0. MS (ESI) calcd for $\text{C}_{17}\text{H}_{17}\text{NO}_2$ (m/z), 267.12; found, 268.14 [M + H]⁺.

2-(Cyclohexylmethyl)furo[2,3-*c*]quinoline 5-Oxide (7m). Solid (160 mg, 84%). ^1H NMR (500 MHz, CDCl_3) δ 8.87 (s, 1H), 8.84 (dd, 1H), 8.09–8.05 (m, 1H), 7.76–7.69 (m, 2H), 6.86 (d, J = 0.7 Hz, 1H), 2.76 (d, J = 6.8 Hz, 2H), 1.90–1.52 (m, 6H), 1.33–1.14 (m, 3H), 1.08–0.97 (m, 2H). ^{13}C NMR (126 MHz, CDCl_3) δ 162.9, 147.2, 138.7, 128.9, 128.5, 124.5, 124.3, 123.7, 122.8, 121.0, 102.3, 37.3, 36.6, 33.3, 29.9, 26.4, 26.2. MS (ESI) calcd for $\text{C}_{18}\text{H}_{19}\text{NO}_2$ (m/z), 281.14; found, 282.16 [M + H]⁺.

2-Phenylfuro[2,3-*c*]quinoline 5-Oxide (7n). White solid (73 mg, 68%). ^1H NMR (500 MHz, CDCl_3) δ 8.96 (d, J = 0.7 Hz, 1H), 8.89–8.85 (m, 1H), 8.17 (ddd, J = 3.2, 2.2, 0.5 Hz, 1H), 7.94–7.90 (m, 2H), 7.80–7.74 (m, 2H), 7.53–7.49 (m, 2H), 7.47 (d, J = 0.9 Hz, 1H), 7.46–7.42 (m, 1H). ^{13}C NMR (126 MHz, CDCl_3) δ 159.6, 147.5, 139.1, 129.9, 129.3, 129.3, 129.2, 128.8, 125.3, 124.5, 124.4, 124.3, 122.9, 121.2, 100.2. MS (ESI) calcd for $\text{C}_{17}\text{H}_{11}\text{NO}_2$ (m/z), 261.08; found, 262.09 [M + H]⁺.

2-Benzylfuro[2,3-*c*]quinoline 5-Oxide (7o). White solid (96 mg 90%). ^1H NMR (500 MHz, CDCl_3) δ 8.85 (d, J = 0.6 Hz, 1H), 8.83 (dd, 1H), 8.04–8.01 (m, 1H), 7.75–7.67 (m, 2H), 7.38 (ddd, J = 7.2, 4.4, 1.6 Hz, 2H), 7.35–7.30 (m, 3H), 6.82 (d, J = 0.9 Hz, 1H), 4.21 (s, 2H). ^{13}C NMR (126 MHz, CDCl_3) δ 162.0, 147.5, 138.9, 136.1, 129.1, 129.1, 129.0, 128.6, 127.4, 124.5, 124.2, 123.8, 122.8, 121.1, 102.7, 35.3. MS (ESI) calcd for $\text{C}_{18}\text{H}_{13}\text{NO}_2$ (m/z), 275.10; found, 276.11 [M + H]⁺.

2-(Hydroxymethyl)furo[2,3-*c*]quinoline 5-Oxide (7p). Yellow solid (77 mg, 79%). ^1H NMR (500 MHz, MeOD) δ 9.15 (s, 1H), 8.72 (dd, J = 7.9, 1.8 Hz, 1H), 8.38–8.31 (m, 1H), 7.91–7.82 (m, 2H), 7.43 (d, J = 0.6 Hz, 1H), 4.82 (s, 2H). ^{13}C NMR (126 MHz, MeOD) δ 165.1, 148.4, 139.0, 130.7, 130.7, 127.8, 127.0, 125.9, 124.2, 120.9, 103.9, 57.9. MS (ESI) calcd for $\text{C}_{12}\text{H}_9\text{NO}_3$ (m/z), 215.10; found, 216.07 [M + H]⁺.

2-(2-Hydroxyethyl)furo[2,3-*c*]quinoline 5-Oxide (7q). White solid (75 mg, 78%). ^1H NMR (500 MHz, MeOD) δ 9.09 (d, J = 0.5 Hz, 1H), 8.68 (dd, 1H), 8.31–8.27 (m, 1H), 7.88–7.78 (m, 2H), 7.29 (d, J = 0.8 Hz, 1H), 3.99 (t, J = 6.3 Hz, 2H), 3.15 (td, J = 6.3, 0.7 Hz, 2H). ^{13}C NMR (126 MHz, MeOD) δ 164.6, 147.9, 138.8, 130.6, 130.5, 128.5, 126.7, 125.9, 123.9, 120.8, 104.1, 60.5, 33.1. MS (ESI) calcd for $\text{C}_{13}\text{H}_{11}\text{NO}_3$ (m/z), 229.10; found, 230.09 [M + H]⁺.

2-(3-Hydroxypropyl)furo[2,3-*c*]quinoline 5-Oxide (7r). White solid (75 mg, 88%). ^1H NMR (500 MHz, MeOD) δ 9.13 (s, 1H), 8.75–8.69 (m, 1H), 8.38–8.33 (m, 1H), 7.90–7.82 (m, 2H), 7.30 (d, J = 0.9 Hz, 1H), 3.69 (t, J = 6.2 Hz, 2H), 3.06 (t, 2H), 2.10–2.00 (m, 2H). ^{13}C NMR (126 MHz, MeOD) δ 167.0, 148.0, 138.8, 130.6, 130.5, 128.7, 126.7, 126.0, 124.0, 120.8, 103.0, 61.8, 31.5, 26.0. MS (ESI) calcd for $\text{C}_{14}\text{H}_{13}\text{NO}_3$ (m/z), 243.10; found, 244.10 [M + H]⁺.

2-(4-Hydroxybutyl)furo[2,3-*c*]quinoline 5-Oxide (7s). Solid (60 mg, 76%). ^1H NMR (500 MHz, MeOD) δ 8.99 (s, 1H), 8.22–8.18 (m, 1H), 8.09 (dd, J = 8.4, 0.6 Hz, 1H), 7.70 (ddd, J = 8.4, 6.9, 1.6 Hz, 1H), 7.65 (ddd, J = 8.1, 7.0, 1.3 Hz, 1H), 7.17 (d, J = 0.8 Hz, 1H), 3.63 (t, J = 6.4 Hz, 2H), 2.98 (t, 2H), 1.96–1.88 (m, 2H), 1.71–1.63 (m, 2H). ^{13}C NMR (126 MHz, MeOD) δ 165.5, 149.8, 144.7, 136.6, 133.6, 129.5, 128.9, 128.0, 125.1, 124.3, 102.4, 62.4, 33.0, 29.2, 25.2.

MS (ESI) calcd for $\text{C}_{15}\text{H}_{15}\text{NO}_3$ (m/z), 257.10; found, 258.11 [M + H]⁺.

2-(2-Hydroxypropan-2-yl)furo[2,3-*c*]quinoline 5-Oxide (7t). White solid (63 mg 74%). ^1H NMR (500 MHz, MeOD) δ 9.17 (s, 1H), 8.73 (d, 1H), 8.38 (dd, 1H), 7.92–7.83 (m, 2H), 7.42 (d, 1H), 1.70 (s, 6H). ^{13}C NMR (126 MHz, MeOD) δ 171.2, 148.0, 139.0, 130.8, 130.7, 127.9, 127.0, 126.0, 124.3, 120.9, 101.3, 70.0, 29.0. MS (ESI) calcd for $\text{C}_{14}\text{H}_{13}\text{NO}_3$ (m/z), 243.10; found, 244.10 [M + H]⁺.

2-(1-Hydroxy-3-methylbutyl)furo[2,3-*c*]quinoline 5-Oxide (7u). Solid (60 mg, 70%). ^1H NMR (500 MHz, MeOD) δ 9.18 (s, 1H), 8.74 (dd, 1H), 8.40 (dd, 1H), 7.92–7.85 (m, 2H), 7.46 (s, 1H), 4.98 (dd, J = 8.5, 5.1 Hz, 1H), 1.91–1.85 (m, 2H), 1.84–1.78 (m, 1H), 1.02 (dd, J = 6.3, 3.0 Hz, 6H). ^{13}C NMR (126 MHz, MeOD) δ 168.3, 148.1, 139.0, 130.7, 130.7, 127.9, 127.0, 126.0, 124.3, 120.9, 102.8, 66.9, 45.7, 25.7, 23.6, 22.3. MS (ESI) calcd for $\text{C}_{16}\text{H}_{17}\text{NO}_3$ (m/z), 271.12; found, 272.12 [M + H]⁺.

2-(2-Hydroxypropyl)furo[2,3-*c*]quinoline 5-Oxide (7v). Solid (65 mg, 81%). ^1H NMR (500 MHz, MeOD) δ 9.04 (d, J = 0.6 Hz, 1H), 8.63–8.60 (m, 1H), 8.27–8.24 (m, 1H), 7.80–7.72 (m, 2H), 7.23 (d, J = 0.7 Hz, 1H), 4.20–4.11 (m, 1H), 2.97 (ddd, J = 3.9, 2.6, 0.5 Hz, 2H), 1.21 (d, J = 6.2 Hz, 3H). ^{13}C NMR (126 MHz, MeOD) δ 164.5, 148.0, 138.8, 130.6, 130.5, 128.59, 126.8, 126.0, 124.0, 120.8, 104.6, 67.0, 39.2, 23.4. MS (ESI) calcd for $\text{C}_{14}\text{H}_{13}\text{NO}_3$ (m/z), 243.10; found, 244.10 [M + H]⁺.

2-(2-Ethoxyethyl)furo[2,3-*c*]quinoline 5-Oxide (7w). Solid (30 mg, 70%). ^1H NMR (500 MHz, MeOD) δ 9.15 (d, J = 0.7 Hz, 1H), 8.74–8.71 (m, 1H), 8.39–8.35 (m, 1H), 7.91–7.84 (m, 2H), 7.34 (d, J = 0.9 Hz, 1H), 3.89 (t, J = 6.3 Hz, 2H), 3.58 (q, J = 7.0 Hz, 2H), 3.24–3.21 (m, 2H), 1.19 (t, J = 7.0 Hz, 3H). ^{13}C NMR (126 MHz, MeOD) δ 164.7, 147.9, 138.9, 130.6, 130.6, 128.6, 126.8, 126.0, 124.0, 120.8, 103.9, 68.6, 67.4, 30.4, 15.4. MS (ESI) calcd for $\text{C}_{15}\text{H}_{15}\text{NO}_3$ (m/z), 257.10; found, 258.11 [M + H]⁺.

2-((1,3-Dioxoisooindolin-2-yl)methyl)furo[2,3-*c*]quinoline 5-Oxide (7x). Solid (33 mg, 61%). ^1H NMR (500 MHz, DMSO) δ 9.22 (s, 1H), 8.63–8.59 (m, 1H), 8.41–8.36 (m, 1H), 7.97–7.93 (m, 2H), 7.91–7.87 (m, 2H), 7.83–7.76 (m, 2H), 7.67 (d, J = 0.7 Hz, 1H), 5.06 (s, 2H). ^{13}C NMR (126 MHz, DMSO) δ 167.2, 155.4, 147.4, 138.5, 134.8, 131.6, 129.3, 128.6, 124.9, 124.1, 123.5, 122.4, 121.6, 120.0, 104.4, 34.7. MS (ESI) calcd for $\text{C}_{20}\text{H}_{12}\text{N}_2\text{O}_4$ (m/z), 344.08; found, 345.09 [M + H]⁺.

2-((1,3-Dioxoisooindolin-2-yl)ethyl)furo[2,3-*c*]quinoline 5-Oxide (7y). Solid (65 mg, 77%). ^1H NMR (500 MHz, MeOD) δ 8.92 (d, J = 0.7 Hz, 1H), 8.70 (dd, J = 8.2, 1.5 Hz, 1H), 8.21–8.17 (m, 1H), 7.84–7.77 (m, 4H), 7.77–7.73 (m, 2H), 7.19 (d, J = 0.8 Hz, 1H), 4.15 (t, J = 6.7 Hz, 2H), 3.35 (t, J = 7.1, 6.5 Hz, 2H). ^{13}C NMR (126 MHz, MeOD) δ 168.9, 161.8, 147.5, 138.4, 135.0, 134.9, 132.4, 130.0, 130.0, 127.3, 125.8, 125.3, 124.0, 123.9, 123.4, 120.5, 104.0, 36.6, 28.3. MS (ESI) calcd for $\text{C}_{21}\text{H}_{14}\text{N}_2\text{O}_4$ (m/z), 358.10; found, 359.11 [M + H]⁺.

General Procedure for the Installation of the 4-Amino Group. To a stirred solution of N-oxide (0.414 mmol) in CH_2Cl_2 was added benzoylisocyanate (1.24 mmol). The resulting reaction mixture was stirred at 55 °C for 2 h. After the completion of the reaction (monitored by TLC), the solvent was evaporated. The residue was redissolved in MeOH (4 mL), and NaOMe (2.07 mmol) was added and refluxed for 4 h. The solvent was evaporated, and the crude material was purified by flash chromatography using CH_2Cl_2 /MeOH as the eluent. For compounds 8x and 8y, after the reaction with benzoylisocyanate (first step), the solvent was evaporated, and ethylenediamine (2 mL) was added and stirred at 70 °C for 12 h.

Furo[2,3-*c*]quinolin-4-amine (8a). Solid (16 mg, 68%). ^1H NMR (500 MHz, CDCl_3) δ 7.93 (ddd, J = 8.0, 1.5, 0.5 Hz, 1H), 7.81 (ddd, J = 8.4, 1.1, 0.5 Hz, 1H), 7.79 (d, J = 2.0 Hz, 1H), 7.55 (ddd, J = 8.5, 7.0, 1.5 Hz, 1H), 7.38 (ddd, J = 8.1, 7.0, 1.2 Hz, 1H), 7.20 (d, J = 2.0 Hz, 1H), 5.16 (s, 2H). ^{13}C NMR (126 MHz, CDCl_3) δ 146.4, 145.2, 144.3, 139.5, 129.9, 127.8, 126.6, 123.4, 123.1, 120.5, 106.2. HRMS (ESI) calcd for $\text{C}_{11}\text{H}_8\text{N}_2\text{O}$ (m/z), 184.0637; found, 185.0704 [M + H]⁺.

2-Methylfuro[2,3-*c*]quinolin-4-amine (8b). Solid (35 mg, 70%). ^1H NMR (500 MHz, CDCl_3) δ 7.85 (ddd, J = 8.9, 5.0, 0.8 Hz, 2H), 7.55 (ddd, J = 8.4, 7.0, 1.5 Hz, 1H), 7.36 (ddd, J = 8.1, 7.1, 1.2 Hz,

1H), 6.81 (d, J = 1.0 Hz, 1H), 5.88 (s, 2H), 2.57 (d, J = 1.0 Hz, 3H). ^{13}C NMR (126 MHz, CDCl_3) δ 158.3, 144.9, 138.3, 132.0, 131.3, 129.7, 128.0, 125.3, 123.5, 123.1, 102.7, 14.5. HRMS (ESI) calcd for $\text{C}_{12}\text{H}_{10}\text{N}_2\text{O}$ (m/z), 198.0793; found, 199.0859 [$\text{M} + \text{H}]^+$.

2-Propylfuro[2,3-*c*]quinolin-4-amine (8c). Solid (38 mg, 78%). ^1H NMR (500 MHz, CDCl_3) δ 7.88 (dd, J = 8.0, 1.2 Hz, 1H), 7.81–7.76 (m, 1H), 7.52 (ddd, J = 8.4, 7.0, 1.5 Hz, 1H), 7.34 (ddd, J = 8.0, 7.0, 1.1 Hz, 1H), 6.81 (t, J = 0.8 Hz, 1H), 5.12 (s, 2H), 2.89–2.81 (m, 2H), 1.88–1.80 (m, 2H), 1.05 (t, J = 7.4 Hz, 3H). ^{13}C NMR (126 MHz, CDCl_3) δ 161.7, 144.8, 144.1, 138.6, 131.4, 127.6, 126.5, 123.4, 122.8, 120.4, 101.8, 30.7, 21.3, 13.9. HRMS (ESI) calcd for $\text{C}_{14}\text{H}_{14}\text{N}_2\text{O}$ (m/z), 226.1106; found, 227.1183 [$\text{M} + \text{H}]^+$.

2-Butylfuro[2,3-*c*]quinolin-4-amine (8d). Solid (39 mg, 80%). ^1H NMR (500 MHz, CDCl_3) δ 7.87 (ddd, J = 8.0, 1.4, 0.4 Hz, 1H), 7.80–7.76 (m, 1H), 7.52 (ddd, J = 8.4, 7.0, 1.5 Hz, 1H), 7.34 (ddd, J = 8.1, 7.0, 1.2 Hz, 1H), 6.80 (t, J = 0.8 Hz, 1H), 5.11 (s, 2H), 2.90–2.83 (m, 2H), 1.79 (ddd, J = 13.3, 8.5, 6.7 Hz, 2H), 1.51–1.40 (m, 2H), 0.98 (t, J = 7.4 Hz, 3H). ^{13}C NMR (126 MHz, CDCl_3) δ 161.9, 144.8, 144.1, 138.6, 131.3, 127.6, 126.5, 123.4, 122.8, 120.4, 101.7, 30.0, 28.4, 22.4, 13.9. HRMS (ESI) calcd for $\text{C}_{15}\text{H}_{16}\text{N}_2\text{O}$ (m/z), 240.1263; found, 241.1349 [$\text{M} + \text{H}]^+$.

2-Pentylfuro[2,3-*c*]quinolin-4-amine (8e). Solid (34 mg, 69%). ^1H NMR (500 MHz, CDCl_3) δ 7.88 (dd, J = 8.0, 1.1 Hz, 1H), 7.78 (dd, J = 8.4, 0.5 Hz, 1H), 7.52 (ddd, J = 8.4, 7.0, 1.5 Hz, 1H), 7.34 (ddd, J = 8.1, 7.0, 1.2 Hz, 1H), 6.80 (s, 1H), 5.09 (s, 2H), 2.88–2.83 (m, 2H), 1.84–1.77 (m, 2H), 1.46–1.34 (m, 4H), 0.93 (t, J = 7.1 Hz, 3H). ^{13}C NMR (126 MHz, CDCl_3) δ 161.9, 144.8, 144.2, 138.6, 131.3, 127.6, 126.5, 123.4, 122.8, 120.4, 101.7, 31.5, 28.7, 27.6, 22.5, 14.1. HRMS (ESI) calcd for $\text{C}_{16}\text{H}_{18}\text{N}_2\text{O}$ (m/z), 254.1419; found, 255.1496 [$\text{M} + \text{H}]^+$.

2-Hexylfuro[2,3-*c*]quinolin-4-amine (8f). Yellow solid (60 mg, 67%). ^1H NMR (500 MHz, CDCl_3) δ 7.90–7.86 (m, 1H), 7.79 (dd, J = 8.4, 0.5 Hz, 1H), 7.52 (ddd, J = 8.5, 7.0, 1.5 Hz, 1H), 7.34 (ddd, J = 8.1, 7.0, 1.2 Hz, 1H), 6.80 (s, 1H), 5.21 (s, 2H), 2.86 (t, 2H), 1.84–1.76 (m, 2H), 1.47–1.39 (m, 2H), 1.38–1.29 (m, 4H), 0.91 (t, J = 7.1 Hz, 3H). ^{13}C NMR (126 MHz, CDCl_3) δ 161.8, 144.8, 138.4, 131.2, 128.6, 127.5, 126.2, 123.3, 122.7, 120.2, 101.5, 31.5, 28.9, 28.6, 27.8, 22.6, 14.1. HRMS (ESI) calcd for $\text{C}_{17}\text{H}_{20}\text{N}_2\text{O}$ (m/z), 268.1576; found, 269.1658 [$\text{M} + \text{H}]^+$.

2-Isobutylfuro[2,3-*c*]quinolin-4-amine (8g). Solid (55 mg, 70%). ^1H NMR (500 MHz, CDCl_3) δ 7.87 (ddd, J = 7.9, 1.4, 0.4 Hz, 1H), 7.80 (ddd, J = 8.5, 1.1, 0.5 Hz, 1H), 7.53 (ddd, J = 8.4, 7.0, 1.5 Hz, 1H), 7.34 (ddd, J = 8.1, 7.0, 1.2 Hz, 1H), 6.81 (s, 1H), 5.36 (s, 2H), 2.73 (dd, J = 7.1, 0.6 Hz, 2H), 2.15 (dp, J = 13.6, 6.8 Hz, 1H), 1.02 (d, J = 6.7 Hz, 6H). ^{13}C NMR (126 MHz, CDCl_3) δ 161.1, 144.9, 143.8, 138.6, 131.4, 127.6, 126.2, 123.4, 122.8, 120.2, 102.7, 37.9, 28.0, 22.6. HRMS (ESI) calcd for $\text{C}_{15}\text{H}_{16}\text{N}_2\text{O}$ (m/z), 240.1263; found, 241.1337 [$\text{M} + \text{H}]^+$.

2-(*tert*-Butyl)furo[2,3-*c*]quinolin-4-amine (8h). ^1H NMR (500 MHz, CDCl_3) δ 7.89 (ddd, J = 8.0, 1.5, 0.5 Hz, 1H), 7.79 (dd, J = 8.4, 0.5 Hz, 1H), 7.53 (ddd, J = 8.4, 7.0, 1.5 Hz, 1H), 7.35 (ddd, J = 8.1, 7.0, 1.2 Hz, 1H), 6.80 (s, 1H), 5.27 (s, 2H), 1.45 (s, 9H). ^{13}C NMR (126 MHz, CDCl_3) δ 169.8, 144.8, 143.6, 138.4, 131.3, 127.7, 126.1, 123.4, 123.0, 120.4, 99.0, 33.6, 29.2. HRMS (ESI) calcd for $\text{C}_{15}\text{H}_{16}\text{N}_2\text{O}$ (m/z), 240.1263; found, 241.1342 [$\text{M} + \text{H}]^+$.

2-Isopentylfuro[2,3-*c*]quinolin-4-amine (8i). Solid (35 mg, 70%). ^1H NMR (500 MHz, CDCl_3) δ 7.87 (dd, J = 8.0, 1.0 Hz, 1H), 7.79 (dd, J = 8.4, 0.5 Hz, 1H), 7.53 (ddd, J = 8.4, 7.0, 1.5 Hz, 1H), 7.35 (ddd, J = 8.1, 7.1, 1.2 Hz, 1H), 6.81 (d, J = 0.8 Hz, 1H), 5.45–5.18 (m, 2H), 2.87 (t, 2H), 1.73–1.64 (m, 3H), 0.99 (d, J = 6.4 Hz, 6H). ^{13}C NMR (126 MHz, CDCl_3) δ 162.5, 144.8, 138.3, 131.6, 128.8, 127.8, 126.0, 123.4, 123.0, 120.2, 101.6, 36.8, 27.8, 26.7, 22.5. HRMS (ESI) calcd for $\text{C}_{16}\text{H}_{18}\text{N}_2\text{O}$ (m/z), 254.1419; found, 255.1496 [$\text{M} + \text{H}]^+$.

2-Cyclopropylfuro[2,3-*c*]quinolin-4-amine (8j). Solid (28 mg, 74%). ^1H NMR (500 MHz, CDCl_3) δ 7.85 (dd, J = 8.0, 1.1 Hz, 1H), 7.77 (dd, J = 8.4, 0.5 Hz, 1H), 7.52 (ddd, J = 8.4, 7.0, 1.5 Hz, 1H), 7.33 (ddd, J = 8.1, 7.0, 1.1 Hz, 1H), 6.78–6.75 (m, 1H), 5.15–5.03 (m, 2H), 2.14 (tt, J = 8.4, 5.1 Hz, 1H), 1.10 (tdd, J = 11.1, 7.0, 4.3 Hz, 2H), 1.05–0.99 (m, 2H). ^{13}C NMR (126 MHz, CDCl_3) δ 162.7, 144.5, 143.9, 137.9, 131.5, 127.5, 126.3, 123.3, 122.7, 120.1, 99.9, 29.7,

9.6, 8.0. HRMS (ESI) calcd for $\text{C}_{14}\text{H}_{12}\text{N}_2\text{O}$ (m/z), 224.0950; found, 225.1016 [$\text{M} + \text{H}]^+$.

2-Cyclopentylfuro[2,3-*c*]quinolin-4-amine (8k). Solid (40 mg, 68%). ^1H NMR (500 MHz, CDCl_3) δ 7.87 (dd, J = 8.0, 1.1 Hz, 1H), 7.78 (dd, J = 8.4, 0.5 Hz, 1H), 7.52 (ddd, J = 8.4, 7.0, 1.5 Hz, 1H), 7.34 (ddd, J = 8.1, 7.0, 1.2 Hz, 1H), 6.81 (d, J = 0.9 Hz, 1H), 5.13 (s, 2H), 3.35–3.27 (m, 1H), 2.20–2.11 (m, 2H), 1.89–1.82 (m, 3H), 1.79–1.70 (m, 3H). ^{13}C NMR (126 MHz, CDCl_3) δ 165.5, 144.8, 144.0, 138.5, 131.3, 127.6, 126.4, 123.4, 122.8, 120.4, 100.2, 39.3, 32.1, 29.9, 25.5. HRMS (ESI) calcd for $\text{C}_{16}\text{H}_{16}\text{N}_2\text{O}$ (m/z), 252.1263; found, 253.1338 [$\text{M} + \text{H}]^+$.

2-(Cyclopentylmethyl)furo[2,3-*c*]quinolin-4-amine (8l). Solid (44 mg, 75%). ^1H NMR (500 MHz, CDCl_3) δ 7.88 (ddd, J = 7.9, 1.4, 0.4 Hz, 1H), 7.78 (dd, J = 8.4, 0.6 Hz, 1H), 7.52 (ddd, J = 8.4, 7.0, 1.5 Hz, 1H), 7.34 (ddd, J = 8.1, 7.0, 1.2 Hz, 1H), 6.81 (s, 1H), 5.09 (s, 2H), 2.88–2.83 (m, 2H), 2.40–2.29 (m, 1H), 1.90–1.82 (m, 2H), 1.69 (ddd, J = 7.1, 6.7, 4.7 Hz, 2H), 1.64–1.54 (m, 2H), 1.36–1.26 (m, 2H). ^{13}C NMR (126 MHz, CDCl_3) δ 161.6, 144.8, 144.1, 138.6, 131.3, 127.6, 126.5, 123.4, 122.8, 120.4, 102.1, 38.9, 34.8, 32.7, 25.2. HRMS (ESI) calcd for $\text{C}_{17}\text{H}_{18}\text{N}_2\text{O}$ (m/z), 266.1419; found, 267.1495 [$\text{M} + \text{H}]^+$.

2-(Cyclohexylmethyl)furo[2,3-*c*]quinolin-4-amine (8m). White solid (75 mg, 71%). ^1H NMR (500 MHz, CDCl_3) δ 7.89–7.86 (m, 1H), 7.78 (dd, J = 8.4, 0.5 Hz, 1H), 7.52 (ddd, J = 8.4, 7.0, 1.5 Hz, 1H), 7.34 (ddd, J = 8.1, 7.1, 1.1 Hz, 1H), 6.79 (s, 1H), 5.19 (s, 2H), 2.74 (d, J = 6.6 Hz, 2H), 1.81–1.65 (m, 6H), 1.32–1.14 (m, 4H), 1.04 (qd, J = 12.9, 2.8 Hz, 1H). ^{13}C NMR (126 MHz, CDCl_3) δ 160.8, 144.9, 144.1, 138.6, 131.3, 127.6, 126.4, 123.4, 122.8, 120.4, 102.7, 37.4, 36.6, 33.3, 26.4, 26.3. HRMS (ESI) calcd for $\text{C}_{18}\text{H}_{20}\text{N}_2\text{O}$ (m/z), 280.1576; found, 281.1656 [$\text{M} + \text{H}]^+$.

2-Phenylfuro[2,3-*c*]quinolin-4-amine (8n). Solid (30 mg, 75%). ^1H NMR (500 MHz, CDCl_3) δ 7.97 (ddd, J = 8.0, 1.4, 0.4 Hz, 1H), 7.94–7.90 (m, 2H), 7.83–7.79 (m, 1H), 7.56 (ddd, J = 8.4, 7.0, 1.5 Hz, 1H), 7.53–7.48 (m, 2H), 7.45–7.41 (m, 2H), 7.39 (ddd, J = 8.1, 7.0, 1.2 Hz, 1H), 5.23 (s, 2H). ^{13}C NMR (126 MHz, CDCl_3) δ 157.8, 145.0, 144.4, 139.0, 131.7, 129.9, 129.5, 129.1, 127.9, 126.7, 125.3, 123.4, 123.1, 120.3, 100.8. HRMS (ESI) calcd for $\text{C}_{17}\text{H}_{12}\text{N}_2\text{O}$ (m/z), 260.0950; found, 261.1023 [$\text{M} + \text{H}]^+$.

2-Benzylfuro[2,3-*c*]quinolin-4-amine (8o). Solid (45 mg, 65%). ^1H NMR (500 MHz, CDCl_3) δ 7.86–7.82 (m, 1H), 7.77 (dd, J = 8.4, 0.6 Hz, 1H), 7.52 (ddd, J = 8.4, 7.0, 1.5 Hz, 1H), 7.40–7.35 (m, 2H), 7.35–7.28 (m, 4H), 6.79 (t, J = 0.9 Hz, 1H), 5.10 (s, 2H), 4.21 (s, 2H). ^{13}C NMR (126 MHz, CDCl_3) δ 159.8, 144.9, 144.2, 139.0, 136.7, 131.2, 129.1, 129.0, 127.7, 127.2, 126.5, 123.4, 122.9, 120.4, 103.2, 35.2. HRMS (ESI) calcd for $\text{C}_{18}\text{H}_{14}\text{N}_2\text{O}$ (m/z), 274.1106; found, 275.1182 [$\text{M} + \text{H}]^+$.

(4-Aminofuro[2,3-*c*]quinolin-2-yl)methanol (8p). White solid (12 mg, 67%). ^1H NMR (500 MHz, DMSO) δ 8.00 (dd, J = 7.9, 1.2 Hz, 1H), 7.59 (d, J = 7.9 Hz, 1H), 7.45 (ddd, J = 8.4, 7.0, 1.5 Hz, 1H), 7.31 (s, 1H), 7.25 (ddd, J = 8.0, 7.0, 1.1 Hz, 1H), 6.78 (s, 2H), 4.67 (s, 2H). ^{13}C NMR (126 MHz, DMSO) δ 159.9, 146.1, 144.4, 138.6, 129.6, 127.1, 125.5, 123.5, 121.5, 119.4, 103.0, 56.4. HRMS (ESI) calcd for $\text{C}_{12}\text{H}_{10}\text{N}_2\text{O}_2$ (m/z), 214.0742; found, 215.0805 [$\text{M} + \text{H}]^+$.

2-(4-Aminofuro[2,3-*c*]quinolin-2-yl)ethanol (8q). White solid (20 mg, 65%). ^1H NMR (500 MHz, CDCl_3) δ 7.72 (d, J = 8.3 Hz, 1H), 7.65 (dd, J = 8.0, 1.1 Hz, 1H), 7.50 (ddd, J = 8.4, 5.9, 1.5 Hz, 1H), 7.30–7.26 (m, 1H), 6.79 (s, 1H), 5.28 (s, 2H), 4.10 (t, J = 6.0 Hz, 2H), 3.11 (t, J = 5.8 Hz, 2H). ^{13}C NMR (126 MHz, CDCl_3) δ 158.9, 144.6, 143.0, 138.3, 131.3, 127.8, 125.7, 123.4, 123.0, 119.8, 103.6, 60.5, 32.5. HRMS (ESI) calcd for $\text{C}_{13}\text{H}_{12}\text{N}_2\text{O}_2$ (m/z), 228.0899; found, 229.0962 [$\text{M} + \text{H}]^+$.

3-(4-Aminofuro[2,3-*c*]quinolin-2-yl)propan-1-ol (8r). Solid (70 mg, 75%). ^1H NMR (500 MHz, CDCl_3) δ 7.86 (dd, J = 8.0, 1.3 Hz, 1H), 7.78 (d, J = 8.3 Hz, 1H), 7.52 (ddd, J = 8.4, 7.1, 1.5 Hz, 1H), 7.37–7.32 (m, 1H), 6.84 (s, 1H), 5.24 (s, 2H), 3.78 (t, J = 6.2 Hz, 2H), 3.00 (t, J = 7.5 Hz, 2H), 2.12–2.03 (m, 2H). ^{13}C NMR (126 MHz, CDCl_3) δ 161.1, 144.8, 143.8, 138.6, 131.4, 127.8, 126.2, 123.4, 123.0, 120.2, 102.1, 61.8, 30.8, 25.1. HRMS (ESI) calcd for $\text{C}_{14}\text{H}_{14}\text{N}_2\text{O}_2$ (m/z), 242.1055; found, 243.1120 [$\text{M} + \text{H}]^+$.

4-(4-Aminofuro[2,3-*c*]quinolin-2-yl)butan-1-ol (8s). Solid (28 mg, 70%). ^1H NMR (500 MHz, MeOD) δ 7.95–7.91 (m, 1H), 7.65 (dd, J = 8.4, 0.5 Hz, 1H), 7.49 (ddd, J = 8.5, 7.0, 1.5 Hz, 1H), 7.31 (ddd, J = 8.1, 7.1, 1.1 Hz, 1H), 7.01 (s, 1H), 3.63 (t, J = 6.5 Hz, 2H), 2.94 (t, J = 7.5 Hz, 2H), 1.95–1.87 (m, 2H), 1.70–1.63 (m, 2H). ^{13}C NMR (126 MHz, MeOD) δ 163.9, 147.2, 144.2, 139.5, 133.0, 128.8, 125.5, 124.6, 123.7, 120.8, 102.8, 62.5, 33.0, 29.1, 25.3. HRMS (ESI) calcd for $\text{C}_{15}\text{H}_{16}\text{N}_2\text{O}_2$ (m/z), 256.1212; found, 257.1282 [$\text{M} + \text{H}]^+$.

2-(4-Aminofuro[2,3-*c*]quinolin-2-yl)propan-2-ol (8t). Solid (46 mg, 76%). ^1H NMR (500 MHz, CDCl_3) δ 7.77–7.71 (m, 2H), 7.52–7.47 (m, 1H), 7.29 (ddd, J = 8.1, 7.1, 1.0 Hz, 1H), 6.86 (s, 1H), 1.72 (s, 6H). ^{13}C NMR (126 MHz, CDCl_3) δ 165.5, 145.1, 143.3, 138.4, 130.8, 127.9, 125.8, 123.3, 123.1, 120.0, 100.3, 77.2, 69.2, 29.0. HRMS (ESI) calcd for $\text{C}_{14}\text{H}_{14}\text{N}_2\text{O}_2$ (m/z), 242.1055; found, 243.1123 [$\text{M} + \text{H}]^+$.

1-(4-Aminofuro[2,3-*c*]quinolin-2-yl)-3-methylbutan-1-ol (8u). Solid (35 mg, 77%). ^1H NMR (500 MHz, MeOD) δ 8.00 (d, 1H), 7.67 (d, J = 8.2 Hz, 1H), 7.53 (ddd, J = 8.4, 7.1, 1.4 Hz, 1H), 7.39–7.33 (m, 1H), 7.24 (d, J = 2.6 Hz, 1H), 4.96 (t, J = 6.7 Hz, 1H), 1.92–1.80 (m, 3H), 1.02 (dd, J = 6.2, 4.0 Hz, 6H). ^{13}C NMR (126 MHz, MeOD) δ 165.7, 147.3, 143.5, 132.8, 130.6, 129.2, 125.0, 124.7, 124.1, 120.6, 102.9, 66.9, 45.8, 25.7, 23.6, 22.3. HRMS (ESI) calcd for $\text{C}_{16}\text{H}_{18}\text{N}_2\text{O}_2$ (m/z), 270.1368; found, 271.1468 [$\text{M} + \text{H}]^+$.

1-(4-Aminofuro[2,3-*c*]quinolin-2-yl)propan-2-ol (8v). Solid (30 mg, 73%). ^1H NMR (500 MHz, MeOD) δ 7.96 (dd, J = 8.2, 1.3 Hz, 1H), 7.65 (dd, J = 8.4, 0.4 Hz, 1H), 7.50 (ddd, J = 8.5, 7.1, 1.5 Hz, 1H), 7.33 (ddd, J = 8.1, 7.1, 1.1 Hz, 1H), 7.10 (s, 1H), 4.29–4.22 (m, 1H), 3.05–3.01 (m, 2H), 1.30 (d, J = 6.2 Hz, 3H). ^{13}C NMR (126 MHz, MeOD) δ 161.3, 147.2, 144.0, 133.0, 130.4, 128.9, 125.3, 124.6, 123.8, 120.7, 104.4, 67.2, 39.0, 23.4. HRMS (ESI) calcd for $\text{C}_{14}\text{H}_{14}\text{N}_2\text{O}_2$ (m/z), 242.1055; found, 243.1121 [$\text{M} + \text{H}]^+$.

2-(2-Ethoxyethyl)furo[2,3-*c*]quinolin-4-amine (8w). Solid (15 mg, 71%). ^1H NMR (500 MHz, MeOD) δ 8.01 (ddd, J = 8.0, 2.3, 1.2 Hz, 1H), 7.68 (d, J = 8.2 Hz, 1H), 7.57 (t, J = 7.3 Hz, 1H), 7.45–7.38 (m, 1H), 7.16 (s, 1H), 3.89 (t, J = 6.4 Hz, 2H), 3.58 (q, J = 7.0 Hz, 2H), 3.20 (dt, J = 6.5, 3.1 Hz, 2H), 1.20 (t, J = 7.0 Hz, 3H). ^{13}C NMR (126 MHz, MeOD) δ 163.1, 146.51, 134.2, 133.1, 130.6, 129.7, 129.2, 125.0, 124.7, 123.3, 104.2, 68.9, 67.4, 30.3, 15.4. HRMS (ESI) calcd for $\text{C}_{15}\text{H}_{16}\text{N}_2\text{O}_2$ (m/z), 256.1212; found, 257.1280 [$\text{M} + \text{H}]^+$.

2-(Aminomethyl)furo[2,3-*c*]quinolin-4-amine (8x). Solid (24 mg, 65%). ^1H NMR (500 MHz, MeOD) δ 7.93 (dd, J = 8.0, 1.1 Hz, 1H), 7.65 (dd, J = 8.4, 0.4 Hz, 1H), 7.49 (ddd, J = 8.4, 7.0, 1.5 Hz, 1H), 7.31 (ddd, J = 8.1, 7.1, 1.1 Hz, 1H), 7.15 (s, 1H), 4.03 (s, 2H). ^{13}C NMR (126 MHz, MeOD) δ 162.7, 147.6, 145.0, 140.0, 132.4, 128.7, 126.0, 124.5, 123.6, 121.0, 102.9, 39.8. HRMS (ESI) calcd for $\text{C}_{12}\text{H}_{11}\text{N}_3\text{O}$ (m/z), 213.0902; found, 214.0967 [$\text{M} + \text{H}]^+$.

2-(2-Aminoethyl)furo[2,3-*c*]quinolin-4-amine (8y). Solid (25 mg, 66%). ^1H NMR (500 MHz, MeOD) δ 7.94 (dd, J = 8.0, 1.1 Hz, 1H), 7.64 (dd, J = 8.4, 0.5 Hz, 1H), 7.48 (ddd, J = 8.5, 7.0, 1.5 Hz, 1H), 7.30 (ddd, J = 8.1, 7.1, 1.1 Hz, 1H), 7.07 (s, 1H), 3.14–3.02 (m, 4H). ^{13}C NMR (126 MHz, MeOD) δ 161.1, 147.4, 145.0, 140.0, 132.6, 128.6, 126.0, 124.5, 123.5, 120.9, 103.7, 40.9, 32.7. HRMS (ESI) calcd for $\text{C}_{13}\text{H}_{13}\text{N}_3\text{O}$ (m/z), 227.1059; found, 228.1121 [$\text{M} + \text{H}]^+$.

Compound 10 was synthesized in a similar manner as compound 5.

3-*lodoquinolin-4-ol (10).* Solid (1.6 g). ^1H NMR (500 MHz, DMSO) δ 11.19 (s, 1H), 8.50 (s, 1H), 7.98–7.85 (m, 2H), 7.65–7.60 (m, 1H), 7.60–7.55 (m, 1H). ^{13}C NMR (126 MHz, DMSO) δ 152.2, 142.6, 141.3, 130.9, 129.9, 129.2, 128.5, 126.6, 94.5. MS (ESI) calcd for $\text{C}_9\text{H}_6\text{INO}$ (m/z), 270.95; found, 271.96 [$\text{M} + \text{H}]^+$.

Compounds 11a–11c were synthesized in a similar manner as compound 6c.

2-*Propylfuro[3,2-*c*]quinoline (11a).* Solid (55 mg, 71%). ^1H NMR (500 MHz, CDCl_3) δ 9.10 (s, 1H), 8.28–8.23 (m, 1H), 8.19 (dd, J = 8.0, 0.8 Hz, 1H), 7.67 (ddd, J = 8.5, 6.9, 1.6 Hz, 1H), 7.61 (ddd, J = 8.1, 7.0, 1.2 Hz, 1H), 6.60 (t, J = 0.9 Hz, 1H), 2.91–2.86 (m, 2H), 1.90–1.81 (m, 2H), 1.06 (t, J = 7.4 Hz, 3H). ^{13}C NMR (126 MHz, CDCl_3) δ 160.1, 155.1, 145.4, 145.2, 129.8, 127.8, 126.8, 121.6, 119.9, 117.3, 101.4, 30.5, 21.3, 13.9. MS (ESI) calcd for $\text{C}_{14}\text{H}_{13}\text{NO}$ (m/z), 211.10; found, 212.11 [$\text{M} + \text{H}]^+$.

2-*Butylfuro[3,2-*c*]quinoline (11b).* Solid (258 mg, 69%). ^1H NMR (500 MHz, CDCl_3) δ 9.13 (s, 1H), 8.25 (dd, J = 7.9, 1.6 Hz, 2H), 7.68–7.59 (m, 2H), 6.59 (t, J = 0.8 Hz, 1H), 2.94–2.87 (m, 2H), 1.81 (ddd, J = 15.2, 8.4, 6.7 Hz, 2H), 1.53–1.42 (m, 2H), 0.99 (t, J = 7.4 Hz, 3H). ^{13}C NMR (126 MHz, CDCl_3) δ 160.5, 155.1, 145.4, 145.3, 129.9, 127.9, 126.8, 121.7, 119.9, 117.3, 101.3, 30.0, 28.3, 22.4, 13.9. MS (ESI) calcd for $\text{C}_{15}\text{H}_{15}\text{NO}$ (m/z), 225.11; found, 226.13 [$\text{M} + \text{H}]^+$.

2-*Phenylfuro[3,2-*c*]quinoline (11c).* Solid (68 mg, 75%). ^1H NMR (500 MHz, CDCl_3) δ 9.18 (s, 1H), 8.38 (dd, J = 8.1, 1.2 Hz, 1H), 8.22 (d, J = 8.1 Hz, 1H), 7.98–7.93 (m, 2H), 7.74–7.64 (m, 2H), 7.51 (t, J = 7.7 Hz, 2H), 7.44–7.39 (m, 1H), 7.21 (s, 1H). ^{13}C NMR (126 MHz, CDCl_3) δ 156.6, 155.3, 145.9, 145.5, 130.0, 129.9, 129.1, 129.1, 128.3, 127.1, 125.1, 122.05, 120.1, 117.3, 100.6. MS (ESI) calcd for $\text{C}_{17}\text{H}_{11}\text{NO}$ (m/z), 245.10; found, 246.09 [$\text{M} + \text{H}]^+$.

Compounds 12a–12c were synthesized in a similar manner as compound 7b.

2-*Propylfuro[3,2-*c*]quinoline 5-oxide (12a).* Solid (88 mg, 82%). ^1H NMR (500 MHz, CDCl_3) δ 8.87–8.82 (m, 1H), 8.79 (s, 1H), 8.25–8.20 (m, 1H), 7.76–7.70 (m, 2H), 6.51 (t, J = 0.9 Hz, 1H), 2.89–2.83 (m, 2H), 1.89–1.80 (m, 2H), 1.06 (t, J = 7.4 Hz, 3H). ^{13}C NMR (126 MHz, CDCl_3) δ 162.2, 147.4, 138.7, 130.7, 129.1, 128.8, 121.3, 120.9, 120.6, 117.9, 101.2, 30.5, 21.2, 13.9. MS (ESI) calcd for $\text{C}_{14}\text{H}_{13}\text{NO}_2$ (m/z), 227.10; found, 228.10 [$\text{M} + \text{H}]^+$.

2-*Butylfuro[3,2-*c*]quinoline 5-oxide (12b).* Yellow solid (100 mg, 79%). ^1H NMR (500 MHz, CDCl_3) δ 8.88–8.82 (m, 1H), 8.79 (s, 1H), 8.26–8.20 (m, 1H), 7.76–7.70 (m, 2H), 6.51 (t, J = 0.9 Hz, 1H), 2.91–2.85 (m, 2H), 1.83–1.76 (m, 2H), 1.51–1.43 (m, 2H), 0.99 (t, J = 7.4 Hz, 3H). ^{13}C NMR (126 MHz, CDCl_3) δ 162.4, 147.4, 138.7, 130.7, 129.1, 128.8, 121.3, 120.9, 120.6, 117.9, 101.1, 29.9, 28.3, 22.4, 13.9. MS (ESI) calcd for $\text{C}_{15}\text{H}_{15}\text{NO}_2$ (m/z), 241.11; found, 242.12 [$\text{M} + \text{H}]^+$.

2-*Phenylfuro[3,2-*c*]quinoline 5-oxide (12c).* Solid (90 mg, 85%). ^1H NMR (500 MHz, CDCl_3) δ 8.90–8.86 (m, 2H), 8.37–8.33 (m, 1H), 7.94–7.90 (m, 2H), 7.78 (dd, J = 6.5, 3.3 Hz, 2H), 7.54–7.49 (m, 2H), 7.46–7.41 (m, 1H), 7.11 (s, 1H). ^{13}C NMR (126 MHz, CDCl_3) δ 158.4, 147.6, 139.3, 130.7, 129.7, 129.4, 129.2, 129.2, 125.2, 121.4, 121.4, 120.8, 118.1, 100.0. MS (ESI) calcd for $\text{C}_{17}\text{H}_{11}\text{NO}_2$ (m/z), 261.10; found, 262.09 [$\text{M} + \text{H}]^+$.

Compounds 13a–13c were synthesized in a similar manner as compound 8a.

2-*Propylfuro[3,2-*c*]quinolin-4-amine (13a).* Solid (35 mg, 71%). ^1H NMR (500 MHz, CDCl_3) δ 8.05 (dd, 1H), 7.76 (d, J = 8.2 Hz, 1H), 7.52 (ddd, J = 8.5, 7.0, 1.5 Hz, 1H), 7.34 (ddd, J = 8.1, 7.0, 1.1 Hz, 1H), 6.40 (t, J = 0.9 Hz, 1H), 5.10 (s, 2H), 2.86–2.81 (m, 2H), 1.87–1.78 (m, 2H), 1.04 (t, J = 7.4 Hz, 3H). ^{13}C NMR (126 MHz, CDCl_3) δ 159.1, 156.1, 151.9, 145.0, 128.2, 126.1, 122.9, 119.8, 114.7, 111.0, 99.7, 30.5, 21.4, 13.9. HRMS (ESI) calcd for $\text{C}_{14}\text{H}_{14}\text{N}_2\text{O}$ (m/z), 226.1106; found, 227.1177 [$\text{M} + \text{H}]^+$.

2-*Butylfuro[3,2-*c*]quinolin-4-amine (13b).* White solid (55 mg, 69%). ^1H NMR (500 MHz, CDCl_3) δ 8.05 (ddd, J = 8.0, 1.5, 0.5 Hz, 1H), 7.79–7.73 (m, 1H), 7.52 (ddd, J = 8.5, 7.0, 1.5 Hz, 1H), 7.34 (ddd, J = 8.1, 7.0, 1.1 Hz, 1H), 6.39 (t, J = 0.9 Hz, 1H), 5.14 (s, 2H), 2.89–2.83 (m, 2H), 1.77 (ddd, J = 13.3, 8.5, 6.6 Hz, 2H), 1.50–1.41 (m, 2H), 0.98 (t, J = 7.4 Hz, 3H). ^{13}C NMR (126 MHz, CDCl_3) δ 159.3, 156.0, 151.9, 144.9, 128.3, 126.0, 123.0, 119.8, 114.7, 111.0, 99.6, 30.1, 28.2, 22.4, 13.9. HRMS (ESI) calcd for $\text{C}_{15}\text{H}_{16}\text{N}_2\text{O}$ (m/z), 240.1263; found, 241.1340 [$\text{M} + \text{H}]^+$.

2-*Phenylfuro[3,2-*c*]quinolin-4-amine (13c).* Solid (33 mg, 67%). ^1H NMR (500 MHz, MeOD) δ 8.93 (ddd, J = 8.0, 1.4, 0.4 Hz, 1H), 8.73 (dd, J = 8.4, 1.2 Hz, 2H), 8.47–8.44 (m, 1H), 8.35–8.31 (m, 1H), 8.31–8.27 (m, 2H), 8.21–8.12 (m, 3H). ^{13}C NMR (126 MHz, MeOD) δ 156.9, 156.5, 154.3, 145.9, 130.9, 129.7, 129.5, 129.4, 125.5, 123.6, 120.6, 114.9, 112.9, 100.7, 49.0. HRMS (ESI) calcd for $\text{C}_{17}\text{H}_{12}\text{N}_2\text{O}$ (m/z), 260.0950; found, 261.1027 [$\text{M} + \text{H}]^+$.

Compound 15 was synthesized in a similar manner as compound 5.

4-*lodoisoquinolin-3-ol (15).* Solid (1.4 g). ^1H NMR (500 MHz, DMSO) δ 8.84 (s, 1H), 7.94 (d, J = 8.2 Hz, 1H), 7.76 (dd, J = 8.5, 0.6 Hz, 1H), 7.73–7.67 (m, 1H), 7.37 (ddd, J = 7.9, 6.8, 0.9 Hz, 1H). ^{13}C

NMR (126 MHz, DMSO) δ 159.8, 149.4, 140.9, 132.8, 128.8, 128.5, 123.8, 123.5. MS (ESI) calcd for C_9H_6INO (*m/z*), 270.95; found, 271.96 [M + H]⁺.

Compound **16** was synthesized in a similar manner as compound **6c**.

2-Butylfuro[2,3-*c*]isoquinoline (16). Solid (68 mg, 81%). ¹H NMR (500 MHz, CDCl₃) δ 8.87 (s, 1H), 8.06 (dd, *J* = 8.5, 0.8 Hz, 2H), 7.74 (ddd, *J* = 8.4, 6.9, 1.2 Hz, 1H), 7.57–7.52 (m, 1H), 6.85 (t, *J* = 0.9 Hz, 1H), 2.93–2.87 (m, 2H), 1.82 (ddd, *J* = 13.3, 8.5, 6.7 Hz, 2H), 1.46 (dq, *J* = 14.8, 7.4 Hz, 2H), 0.98 (t, *J* = 7.4 Hz, 3H). ¹³C NMR (126 MHz, CDCl₃) δ 158.6, 158.3, 146.3, 131.3, 130.2, 128.8, 126.4, 125.2, 123.0, 114.4, 100.5, 29.9, 28.6, 22.4, 14.0. MS (ESI) calcd for $C_{15}H_{15}NO$ (*m/z*), 225.12; found, 226.12 [M + H]⁺.

Compound **17** was synthesized in a similar manner as compound **7b**.

2-Butylfuro[2,3-*c*]isoquinoline 4-Oxide (17). Solid (20 mg, 74%). ¹H NMR (500 MHz, MeOD) δ 8.94 (s, 1H), 8.24 (dd, *J* = 8.3, 0.9 Hz, 1H), 8.08 (d, *J* = 8.4 Hz, 1H), 7.83 (ddd, *J* = 8.3, 7.0, 1.2 Hz, 1H), 7.70 (ddd, *J* = 8.2, 7.0, 1.1 Hz, 1H), 7.30 (t, *J* = 0.9 Hz, 1H), 3.03–2.97 (m, 2H), 1.90–1.83 (m, 2H), 1.54–1.46 (m, 2H), 1.02 (t, *J* = 7.4 Hz, 3H). ¹³C NMR (126 MHz, MeOD) δ 162.3, 134.6, 134.6, 131.8, 131.1, 130.5, 128.9, 128.1, 124.2, 121.7, 103.5, 30.8, 28.9, 23.3, 14.1. MS (ESI) calcd for $C_{15}H_{15}NO_2$ (*m/z*), 241.11; found, 242.11 [M + H]⁺.

Compound **18** was synthesized in a similar manner as compound **8a**.

2-Butylfuro[2,3-*c*]isoquinolin-5-amine (18). Solid (15 mg, 62%). ¹H NMR (500 MHz, MeOD) δ 8.17–8.13 (m, 1H), 7.96 (ddd, *J* = 8.2, 1.1, 0.7 Hz, 1H), 7.69 (ddd, *J* = 8.2, 6.9, 1.1 Hz, 1H), 7.43 (ddd, *J* = 8.3, 6.9, 1.2 Hz, 1H), 6.74 (t, *J* = 0.9 Hz, 1H), 2.82–2.75 (m, 2H), 1.79–1.71 (m, 2H), 1.51–1.41 (m, 2H), 0.99 (t, *J* = 7.4 Hz, 3H). ¹³C NMR (126 MHz, MeOD) δ 158.0, 156.0, 154.4, 134.4, 131.7, 125.9, 124.9, 124.1, 117.0, 106.1, 101.2, 31.3, 29.0, 23.3, 14.2. HRMS (ESI) calcd for $C_{15}H_{16}N_2O$ (*m/z*), 240.1263; found, 241.1350 [M + H]⁺.

1-Bromo-2-butylfuro[2,3-*c*]quinoline (19). To a stirred solution of 2-butylfuro[2,3-*c*]quinoline **7d** (100 mg, 0.44 mmol) in CH₂Cl₂ was added bromine (80 μ L, 1.55 mmol), and the mixture was stirred at room temperature for 6 h. After the completion of the reaction (monitored by TLC), the solvent was evaporated, and the crude material was purified by flash chromatography using CH₂Cl₂/MeOH to furnish **19** as a yellow solid (50 mg, 75%). ¹H NMR (500 MHz, CDCl₃) δ 9.08 (s, 1H), 8.90 (d, *J* = 8.0 Hz, 1H), 8.22 (d, *J* = 8.3 Hz, 1H), 7.71 (ddd, *J* = 8.4, 7.0, 1.5 Hz, 1H), 7.68–7.63 (m, 1H), 2.98–2.92 (m, 2H), 1.84–1.76 (m, 2H), 1.44 (dq, *J* = 14.8, 7.4 Hz, 2H), 0.98 (t, *J* = 7.4 Hz, 3H). ¹³C NMR (126 MHz, CDCl₃) δ 159.4, 147.4, 144.5, 136.2, 130.1, 127.9, 127.7, 126.8, 122.9, 122.3, 94.0, 29.6, 26.6, 22.4, 13.9. MS (ESI) calcd for $C_{15}H_{14}BrNO$ (*m/z*), 303.03; found, 304.04 [M + H]⁺.

Compound **21** was synthesized in a similar manner as compound **8a**.

1-Bromo-2-butylfuro[2,3-*c*]quinolin-4-amine (21). Solid (21 mg, 72%). ¹H NMR (500 MHz, MeOD) δ 8.67 (ddd, *J* = 8.2, 1.4, 0.5 Hz, 1H), 7.68 (ddd, *J* = 8.4, 1.1, 0.5 Hz, 1H), 7.53 (ddd, *J* = 8.5, 7.0, 1.5 Hz, 1H), 7.35 (ddd, *J* = 8.2, 7.0, 1.2 Hz, 1H), 2.97 (t, *J* = 7.5 Hz, 2H), 1.86–1.78 (m, 2H), 1.50–1.41 (m, 2H), 1.00 (t, *J* = 7.4 Hz, 3H). ¹³C NMR (126 MHz, MeOD) δ 159.7, 147.2, 145.3, 138.9, 129.1, 128.5, 126.3, 123.4, 123.1, 120.4, 95.0, 30.7, 27.2, 23.3, 14.1. HRMS (ESI) calcd for $C_{15}H_{15}BrN_2O$ (*m/z*), 318.0368; found, 319.0429 [M + H]⁺.

1-Benzyl-2-butylfuro[2,3-*c*]quinoline (22). To a stirred solution of **19** (50 mg, 0.164 mmol) in 1,4-dioxane were added 2-benzyl-4,4,5,5-tetramethyl-1,3,2-dioxaborolane (54 mg, 0.246 mmol), Pd(dppf)Cl₂ (8 mg, 0.009 mmol), Cs₂CO₃ (160 mg, 0.492 mmol), and 0.1 mL of water. The resulting reaction mixture was stirred at 70 °C under a nitrogen atmosphere for 12 h. After the completion of the reaction (monitored by TLC), the reaction mixture was diluted with water and extracted with ethylacetate (3 \times 10 mL). The combined organic layer was dried over Na₂SO₄ and concentrated under reduced pressure, and the crude material was purified by flash chromatography using CH₂Cl₂/MeOH as the eluent to obtain **22** (24 mg, 92%). ¹H NMR (500 MHz, CDCl₃) δ 9.11 (d, *J* = 5.7 Hz, 1H), 8.19–8.14 (m, 1H), 7.94 (dd, *J* = 8.3, 0.8 Hz, 1H), 7.61–7.54 (m, 1H), 7.44–7.37 (m,

1H), 7.28–7.24 (m, 3H), 7.19 (dd, *J* = 10.3, 4.3 Hz, 2H), 4.38 (s, 2H), 2.91–2.86 (m, 2H), 1.80–1.72 (m, 2H), 1.44–1.35 (m, 2H), 0.93 (t, *J* = 7.4 Hz, 3H). ¹³C NMR (126 MHz, CDCl₃) δ 159.8, 148.3, 144.7, 138.9, 136.5, 136.3, 130.3, 130.1, 128.9, 128.0, 127.4, 126.9, 126.6, 126.5, 123.6, 113.9, 101.0, 30.6, 30.5, 26.4, 22.6, 13.9. MS (ESI) calcd for $C_{22}H_{21}NO$ (*m/z*), 315.20; found, 316.18 [M + H]⁺.

Compound **24** was synthesized in a similar manner as compound **8a**.

1-Benzyl-2-butylfuro[2,3-*c*]quinolin-4-amine (24). Solid (31 mg, 75%). ¹H NMR (500 MHz, CDCl₃) δ 7.79–7.73 (m, 2H), 7.44 (ddd, *J* = 8.4, 7.0, 1.4 Hz, 1H), 7.30–7.23 (m, 3H), 7.23–7.18 (m, 2H), 7.15 (ddd, *J* = 8.2, 7.0, 1.2 Hz, 1H), 5.09 (s, 2H), 4.33 (s, 2H), 2.87–2.81 (m, 2H), 1.73 (ddd, *J* = 13.0, 8.5, 6.7 Hz, 2H), 1.39 (dq, *J* = 14.7, 7.4 Hz, 2H), 0.92 (t, *J* = 7.4 Hz, 3H). ¹³C NMR (126 MHz, CDCl₃) δ 158.4, 144.9, 144.4, 139.1, 138.2, 130.0, 128.8, 128.0 (2C), 127.2 (2C), 126.6, 126.6, 123.4, 122.8, 121.0, 114.7, 30.7, 30.4, 26.3, 22.6, 13.9. HRMS (ESI) calcd for $C_{22}H_{22}N_2O$ (*m/z*), 330.1732; found, 331.1808 [M + H]⁺.

Compounds **27a,b** were synthesized in a similar manner as compound **7b**.

2-Propylfuro[2,3-*c*]pyridine 6-Oxide (27a). Oil (85 mg, 78%). ¹H NMR (500 MHz, CDCl₃) δ 8.48 (s, 1H), 8.08 (dd, *J* = 6.7, 1.5 Hz, 1H), 7.30 (d, *J* = 6.7 Hz, 1H), 6.41 (d, *J* = 0.8 Hz, 1H), 2.75 (t, *J* = 7.5 Hz, 2H), 1.81–1.72 (m, 2H), 1.00 (t, *J* = 7.4 Hz, 3H). ¹³C NMR (126 MHz, CDCl₃) δ 165.3, 152.0, 135.0, 128.5, 124.7, 115.8, 102.0, 30.5, 20.8, 13.8. MS (ESI) calcd for $C_{10}H_{11}NO_2$ (*m/z*), 177.08; found, 178.08 [M + H]⁺.

2-Butylfuro[2,3-*c*]pyridine 6-Oxide (27b). Oil (80 mg, 73%). ¹H NMR (500 MHz, CDCl₃) δ 8.52–8.47 (m, 1H), 8.10 (dd, *J* = 6.7, 1.5 Hz, 1H), 7.31 (d, *J* = 6.7 Hz, 1H), 6.42 (d, *J* = 0.9 Hz, 1H), 2.79 (t, 2H), 1.78–1.67 (m, 2H), 1.48–1.37 (m, 2H), 0.96 (t, *J* = 7.4 Hz, 3H). ¹³C NMR (126 MHz, CDCl₃) δ 165.5, 152.0, 135.1, 128.4, 124.8, 115.8, 101.9, 29.5, 28.3, 22.4, 13.9. MS (ESI) calcd for $C_{11}H_{13}NO_2$ (*m/z*), 191.09; found, 192.10 [M + H]⁺.

Compounds **28a,b** was synthesized in a similar manner as compound **8a**.

2-Propylfuro[2,3-*c*]pyridin-7-amine (28a). Oil (33 mg, 67%). ¹H NMR (500 MHz, CDCl₃) δ 7.80 (d, *J* = 5.5 Hz, 1H), 6.85 (d, *J* = 5.5 Hz, 1H), 6.34 (t, *J* = 0.8 Hz, 1H), 4.67 (s, 2H), 2.79–2.71 (m, 2H), 1.82–1.74 (m, 2H), 1.01 (t, *J* = 7.4 Hz, 3H). ¹³C NMR (126 MHz, CDCl₃) δ 161.8, 144.1, 140.5, 139.2, 135.3, 107.5, 102.4, 30.6, 21.1, 13.9. HRMS (ESI) calcd for $C_{10}H_{12}N_2O$ (*m/z*), 176.0950; found, 177.1067 [M + H]⁺.

2-Butylfuro[2,3-*c*]pyridin-7-amine (28b). Oil (35 mg, 71%). ¹H NMR (500 MHz, CDCl₃) δ 7.80 (d, *J* = 5.5 Hz, 1H), 6.85 (d, *J* = 5.5 Hz, 1H), 6.33 (t, *J* = 0.8 Hz, 1H), 4.68 (s, 2H), 2.80–2.74 (m, 2H), 1.77–1.69 (m, 2H), 1.47–1.38 (m, 2H), 0.96 (t, *J* = 7.4 Hz, 3H). ¹³C NMR (126 MHz, CDCl₃) δ 162.0, 144.0, 140.4, 139.2, 135.3, 107.5, 102.3, 29.8, 28.3, 22.4, 13.9. HRMS (ESI) calcd for $C_{11}H_{14}N_2O$ (*m/z*), 190.1106; found, 191.1231 [M + H]⁺.

Human TLR2, -3, -4, -5, -7, -8, and -9 Reporter-Gene Assays (NF- κ B Induction). The induction of NF- κ B was quantified using human TLR2, -3, -4, -5, -7, -8, and -9-specific HEK-Blue reporter-gene assays as previously described by us.^{17,22,23} HEK293 cells stably cotransfected with the appropriate hTLR, MD2, and secreted alkaline phosphatase (sAP) were maintained in HEK-Blue Selection medium containing zeocin and normocin. The stable expression of secreted alkaline phosphatase (sAP) under the control of the NF- κ B/AP-1 promoters is inducible by appropriate TLR agonists, and extracellular sAP in the supernatant is proportional to the NF- κ B induction. HEK-Blue cells were incubated at a density of \sim 10⁵ cells/mL in a volume of 80 μ L/well in 384-well, flat-bottomed, cell-culture-treated microtiter plates until confluence was achieved, and they were subsequently stimulated with graded concentrations of stimuli. sAP was assayed spectrophotometrically using an alkaline phosphatase-specific chromogen (present in HEK-detection medium as supplied by the vendor) at 620 nm.

Immunoassays for Cytokines. Fresh human peripheral blood mononuclear cells (hPBMC) were isolated from human blood obtained by venipuncture with informed consent and as per

institutional guidelines on Ficoll-Hypaque gradients as described elsewhere.⁵⁹ Aliquots of PBMCs (10^5 cells in $100\ \mu\text{L}/\text{well}$) were stimulated for 12 h with graded concentrations of the test compounds. The supernatants were isolated by centrifugation and were assayed in triplicate using analyte-specific multiplexed cytokine/chemokine bead-array assays as reported by us previously.⁶⁰ PBMC supernatants were also analyzed for 41 chemokines and cytokines (EGF, Eotaxin, FGF-2, Flt-3 ligand, Fractalkine, G-CSF, GM-CSF, GRO, IFN- α 2, IFN- γ , IL-10, IL-12 (p40), IL-12 (p70), IL-13, IL-15, IL-17, IL-1ra, IL-1 α , IL-1 β , IL-2, IL-3, IL-4, IL-5, IL-6, IL-7, IL-8, IL-9, IP-10, MCP-1, MCP-3, MDC (CCL22), MIP-1 α , MIP-1 β , PDGF-AA, PDGF-AB/BB, RANTES, TGF α , TNF- α , TNF- β , VEGF, and sCD40L) using a magnetic bead-based multiplexed assay kit (Milliplex MAP Human Cytokine/Chemokine kit). Data were acquired and processed on a MAGPIX instrument (EMD Millipore, Billerica, MA) with intraassay coefficients of variation ranging from 4 to 8% for the 41 analytes.

Flow-Cytometric Immunostimulation Experiments. CD69 upregulation was determined by flow cytometry using protocols published by us previously.^{17,18} Briefly, heparin-anticoagulated whole blood samples were obtained by venipuncture from healthy human volunteers with informed consent and as per guidelines approved by the University of Kansas Human Subjects Experimentation Committee. Aliquots of whole human blood samples were stimulated with graded concentrations of either **8d** or **2** (used as a reference compound) in a 6-well polystyrene plate and incubated at $37\ ^\circ\text{C}$ in a rotary (100 rpm) incubator for 16.5 h. Negative (endotoxin-free water) controls were included in each experiment. Following incubation, $200\ \mu\text{L}$ aliquots of anticoagulated whole blood were stained with $20\ \mu\text{L}$ of fluorochrome-conjugated antibodies at $37\ ^\circ\text{C}$ in the dark for 30 min. For triple-color flow-cytometry experiments, CD3-PE, CDS6-APC, and CD69-PE-Cy7 were used to analyze CD69 activation in each of the main peripheral blood lymphocyte populations: natural killer lymphocytes (NK cells; CD3 $^-$ CD56 $^+$), cytokine-induced killer phenotype (CIK cells; CD3 $^+$ CD56 $^+$), nominal B lymphocytes (CD3 $^-$ CD56 $^-$), and nominal T lymphocytes (CD3 $^+$ CD56 $^-$). Following the staining, erythrocytes were lysed and leukocytes were fixed in one step by mixing $200\ \mu\text{L}$ of the samples in 4 mL of prewarmed Whole Blood Lyse/Fix Buffer (BD Biosciences, San Jose, CA). After washing the cells twice at 200g for 8 min in saline, the cells were transferred to a 96-well plate. Flow cytometry was performed using a BD FACSAarray instrument in the tricolor mode (tricolor flow experiment) and the two-color mode (two-color flow experiment) for the acquisition of 100 000 gated events. Postacquisition analyses were performed using FlowJo v7.0 software (Treestar, Ashland, OR). Compensation for spillover was computed for each experiment on singly stained samples.

Transcriptomal Profiling of Human PBMCs. Detailed procedures for transcriptomal profiling have been described by us previously.¹⁷ Briefly, fresh human PBMC samples were stimulated with $10\ \mu\text{g}/\text{mL}$ of **8d** and **2** for 2 h, and total RNA was extracted from the treated and negative-control blood samples with a QIAamp RNA Blood Mini Kit (Qiagen). Subsequently, 160 ng of each of the RNA samples was used. The Human Genome GeneChip U133 plus 2.0 oligonucleotide array (Affymetrix, Santa Clara, CA) was employed. Established standard protocols at the KU Genomics Facility were performed for cRNA target preparation, array hybridization, washing, staining, and image scanning. The microarray data was first subjected to quality assessment using the Affymetrix GeneChip Operating Software (GCOS). QC criteria included low background, low noise, detection of the positive controls, and a $5'/3'$ ratio of <3.0 . To facilitate the direct comparison of gene expression data between the different samples, the GeneChip data were first subjected to preprocessing. This step involved scaling (in GCOS) the data from all chips to a target intensity value of 500 and further normalization steps in GeneSpring GX (Agilent Technologies, Santa Clara, CA). Prior to identifying the target genes, genes that were detected as nonexpressed in all samples (i.e., those with absence calls) were filtered out. To identify genes whose expression was changed by our compounds, a fold-change threshold of 2.0 between the compound treatment and the negative control was used.

Molecular Modeling and Induced-Fit Docking. We used quantum mechanics/molecular mechanics (QM/MM) methods^{61,62} for induced-fit docking by calculating the quantum mechanical charges for the ligand, whereas the macromolecule was handled using conventional molecular mechanics force fields. The correct bond orders were assigned, hydrogen atoms were added to the residues, and formal partial charges were assigned to atoms using the OPLS all-atom force field.⁶³ The docking grid was generated using the cocrystallized ligand as the grid center. Ligands were modeled in Schrödinger molecular modeling software (Schrödinger, New York, NY) and were minimized to a gradient of $0.001\ \text{kCal}/\text{Mol}\text{\AA}^2$. The QM charges for the ligands were obtained from Jaguar (Schrödinger) using the 3-21G basis set with the BLYP density functional theory.⁶⁴ Initial docking was performed with Glide^{65,66} using a 0.5 van der Waals (vdW) radius scaling factor for both the ligand and protein. This soft-docking procedure was applied to generate diverse docking solutions, and the top 20 poses for each ligand were retained. Finally, each ligand was redocked into its corresponding structures, and the resulting complexes were ranked according to GlideScore.^{65,66}

■ ASSOCIATED CONTENT

S Supporting Information

¹H and ¹³C spectra of compounds **6c–e**, **7c–e**, **8a**, **8c–e**, **11a**, **11b**, **12a**, **12b**, **13a**, **13b**, **16**, **18**, **19**, **21**, **24**, **27a**, **27b**, **28a**, and **28b** and LC–MS analyses of compounds **8a**, **8c–e**, **13a**, **13b**, **18**, **21**, **24**, **28a**, and **28b**. This material is available free of charge via the Internet at <http://pubs.acs.org>.

■ AUTHOR INFORMATION

Corresponding Author

*Tel: 785-864-1610; Fax: 785-864-1961; E-mail: sdavid@ku.edu.

Notes

The authors declare no competing financial interest.

■ ACKNOWLEDGMENTS

This work was supported by NIH/NIAID contract HSN272200900033C.

■ ABBREVIATIONS:

APCs, antigen-presenting cells; CD69, cluster of differentiation 69; DCs, dendritic cells; EC₅₀, half-maximal effective concentration; ESI-TOF, electrospray ionization-time-of-flight; G-CSF, granulocyte colony-stimulating factor; GRO, growth-related oncogene; HEK, Human embryonic kidney; Ig, immunoglobulin; IFN, interferon; MPL, monophosphoryl lipid A; MIP, macrophage inflammatory protein; MHC, major histocompatibility complex; NK, natural killer; NF- κ B, nuclear factor- κ B; NOD, nucleotide oligomerization domain; sAP, secreted alkaline phosphatase; SAR, structure activity relationship; TNF- α , tumor necrosis factor- α ; Th1, helper T lymphocyte, type 1; Th2, helper T lymphocyte, type 2; Tregs, T-regulatory cells; TGF, transforming growth factor; TLR, toll-like receptor

■ REFERENCES

- (1) Hilleman, M. R. Vaccines in Historic Evolution and Perspective: A Narrative of Vaccine Discoveries. *Vaccine* **2000**, *18*, 1436–1447.
- (2) Nabel, G. J. Designing Tomorrow's Vaccines. *N. Engl. J. Med.* **2013**, *368*, 551–560.
- (3) Lessons from Vaccine History. *Nat. Med.* **2012**, *18*, 1717.
- (4) Pashine, A.; Valiante, N. M.; Ulmer, J. B. Targeting the Innate Immune Response with Improved Vaccine Adjuvants. *Nat. Med.* **2005**, *11*, S63–S68.

(5) Glenny, A. T.; Pope, C. G.; Waddington, H.; Wallace, V. The Antigenic Value of Toxoid Precipitated by Potassium-Alum. *J. Pathol. Bacteriol.* **1926**, *29*, 38–45.

(6) Garcon, N.; Van Mechelen, M. Recent Clinical Experience with Vaccines Using MPL- and QS-21-Containing Adjuvant Systems. *Expert Rev. Vaccines* **2011**, *10*, 471–486.

(7) Relyveld, E. H.; Bizzini, B.; Gupta, R. K. Rational Approaches to Reduce Adverse Reactions in Man to Vaccines Containing Tetanus and Diphtheria Toxoids. *Vaccine* **1998**, *16*, 1016–1023.

(8) Gupta, R. K. Aluminum Compounds As Vaccine Adjuvants. *Adv. Drug Delivery Rev.* **1998**, *32*, 155–172.

(9) Loo, Y. M.; Gale, M., Jr. Immune Signaling by RIG-I-Like Receptors. *Immunity* **2011**, *34*, 680–692.

(10) Kersse, K.; Bertrand, M. J.; Lamkanfi, M.; Vandenabeele, P. NOD-Like Receptors and the Innate Immune System: Coping with Danger, Damage and Death. *Cytokine Growth Factor Rev.* **2011**, *22*, 257–276.

(11) Clarke, T. B.; Weiser, J. N. Intracellular Sensors of Extracellular Bacteria. *Immunol. Rev.* **2011**, *243*, 9–25.

(12) Kumagai, Y.; Takeuchi, O.; Akira, S. Pathogen Recognition by Innate Receptors. *J. Infect. Chemother.* **2008**, *14*, 86–92.

(13) Akira, S. Toll-Like Receptors and Innate Immunity. *Adv. Immunol.* **2001**, *78*, 1–56.

(14) Akira, S.; Takeda, K.; Kaisho, T. Toll-Like Receptors: Critical Proteins Linking Innate and Acquired Immunity. *Nat. Immunol.* **2001**, *2*, 675–680.

(15) Cottalorda, A.; Verschelde, C.; Marcais, A.; Tomkowiak, M.; Musette, P.; Uematsu, S.; Akira, S.; Marvel, J.; Bonnefoy-Berard, N. TLR2 Engagement on CD8 T Cells Lowers the Threshold for Optimal Antigen-Induced T Cell Activation. *Eur. J. Immunol.* **2006**, *36*, 1684–1693.

(16) Kaisho, T.; Akira, S. Toll-Like Receptors As Adjuvant Receptors. *Biochim. Biophys. Acta* **2002**, *1589*, 1–13.

(17) Hood, J. D.; Warshakoon, H. J.; Kimbrell, M. R.; Shukla, N. M.; Malladi, S.; Wang, X.; David, S. A. Immunoprofiling Toll-Like Receptor Ligands: Comparison of Immunostimulatory and Proinflammatory Profiles in Ex Vivo Human Blood Models. *Hum. Vaccines* **2010**, *6*, 1–14.

(18) Warshakoon, H. J.; Hood, J. D.; Kimbrell, M. R.; Malladi, S.; Wu, W. Y.; Shukla, N. M.; Agnihotri, G.; Sil, D.; David, S. A. Potential Adjuvant Properties of Innate Immune Stimuli. *Hum. Vaccines* **2009**, *5*, 381–394.

(19) Agnihotri, G.; Crall, B. M.; Lewis, T. C.; Day, T. P.; Balakrishna, R.; Warshakoon, H. J.; Malladi, S. S.; David, S. A. Structure-Activity Relationships in Toll-Like Receptor 2-Agonists Leading to Simplified Monoacyl Lipopeptides. *J. Med. Chem.* **2011**, *54*, 8148–8160.

(20) Salunke, D. B.; Shukla, N. M.; Yoo, E.; Crall, B. M.; Balakrishna, R.; Malladi, S. S.; David, S. A. Structure-Activity Relationships in Human Toll-like Receptor 2-Specific Monoacyl Lipopeptides. *J. Med. Chem.* **2012**, *55*, 3353–3363.

(21) Wu, W.; Li, R.; Malladi, S. S.; Warshakoon, H. J.; Kimbrell, M. R.; Amolins, M. W.; Ukani, R.; Datta, A.; David, S. A. Structure-Activity Relationships in Toll-Like Receptor-2 Agonistic Diacylthioglycerol Lipopeptides. *J. Med. Chem.* **2010**, *53*, 3198–3213.

(22) Shukla, N. M.; Kimbrell, M. R.; Malladi, S. S.; David, S. A. Regioisomerism-Dependent TLR7 Agonism and Antagonism in an Imidazoquinoline. *Bioorg. Med. Chem. Lett.* **2009**, *19*, 2211–2214.

(23) Shukla, N. M.; Malladi, S. S.; Mutz, C. A.; Balakrishna, R.; David, S. A. Structure-Activity Relationships in Human Toll-Like Receptor 7-Active Imidazoquinoline Analogues. *J. Med. Chem.* **2010**, *53*, 4450–4465.

(24) Shukla, N. M.; Mutz, C. A.; Ukani, R.; Warshakoon, H. J.; Moore, D. S.; David, S. A. Syntheses of Fluorescent Imidazoquinoline Conjugates As Probes of Toll-Like Receptor 7. *Bioorg. Med. Chem. Lett.* **2010**, *20*, 6384–6386.

(25) Shukla, N. M.; Lewis, T. C.; Day, T. P.; Mutz, C. A.; Ukani, R.; Hamilton, C. D.; Balakrishna, R.; David, S. A. Toward Self-Adjuvanting Subunit Vaccines: Model Peptide and Protein Antigens Incorporating Covalently Bound Toll-Like Receptor-7 Agonistic Imidazoquinolines. *Bioorg. Med. Chem. Lett.* **2011**, *21*, 3232–3236.

(26) Shukla, N. M.; Mutz, C. A.; Malladi, S. S.; Warshakoon, H. J.; Balakrishna, R.; David, S. A. Toll-Like Receptor (TLR)-7 and -8 Modulatory Activities of Dimeric Imidazoquinolines. *J. Med. Chem.* **2012**, *55*, 1106–1116.

(27) Kokatla, H. P.; Yoo, E.; Salunke, D. B.; Sil, D.; Ng, C. F.; Balakrishna, R.; Malladi, S. S.; Fox, L. M.; David, S. A. Toll-Like Receptor-8 Agonistic Activities in C2, C4, and C8 Modified Thiazolo[4,5-c]quinolines. *Org. Biomol. Chem.* **2013**, *11*, 1179–1198.

(28) Salunke, D. B.; Yoo, E.; Shukla, N. M.; Balakrishna, R.; Malladi, S. S.; Serafin, K. J.; Day, V. W.; Wang, X.; David, S. A. Structure-Activity Relationships in Human Toll-Like Receptor 8-Active 2,3-Diamino-furo[2,3-c]pyridines. *J. Med. Chem.* **2012**, *55*, 8137–8151.

(29) Agnihotri, G.; Ukani, R.; Malladi, S. S.; Warshakoon, H. J.; Balakrishna, R.; Wang, X.; David, S. A. Structure-Activity Relationships in Nucleotide Oligomerization Domain 1 (Nod1) Agonistic Gamma-Glutamylaminopimelic Acid Derivatives. *J. Med. Chem.* **2011**, *54*, 1490–1510.

(30) Ukani, R.; Lewis, T. C.; Day, T. P.; Wu, W.; Malladi, S. S.; Warshakoon, H. J.; David, S. A. Potent Adjuvant Activity of a CCR1-Agonistic Bis-Quinoline. *Bioorg. Med. Chem. Lett.* **2012**, *22*, 293–295.

(31) Gorden, K. B.; Gorski, K. S.; Gibson, S. J.; Kedl, R. M.; Kieper, W. C.; Qiu, X.; Tomai, M. A.; Alkan, S. S.; Vasilakos, J. P. Synthetic TLR Agonists Reveal Functional Differences between Human TLR7 and TLR8. *J. Immunol.* **2005**, *174*, 1259–1268.

(32) Philbin, V. J.; Levy, O. Immunostimulatory Activity of Toll-Like Receptor 8 Agonists Towards Human Leucocytes: Basic Mechanisms and Translational Opportunities. *Biochem. Soc. Trans.* **2007**, *35*, 1485–1491.

(33) Qin, J.; Yao, J.; Cui, G.; Xiao, H.; Kim, T. W.; Fraczek, J.; Wightman, P.; Sato, S.; Akira, S.; Puel, A.; Casanova, J. L.; Su, B.; Li, X. TLR8-Mediated NF- κ B and JNK Activation are TAK1-Independent and MEKK3-Dependent. *J. Biol. Chem.* **2006**, *281*, 21013–21021.

(34) Levy, O.; Suter, E. E.; Miller, R. L.; Wessels, M. R. Unique Efficacy of Toll-Like Receptor 8 Agonists in Activating Human Neonatal Antigen-Presenting Cells. *Blood* **2006**, *108*, 1284–1290.

(35) Smith, T. R.; Kumar, V. Revival of CD8+ Treg-Mediated Suppression. *Trends Immunol.* **2008**, *29*, 337–342.

(36) Gupta, S.; Shang, W.; Sun, Z. Mechanisms Regulating the Development and Function of Natural Regulatory T Cells. *Arch. Immunol. Ther. Exp.* **2008**, *56*, 85–102.

(37) Cools, N.; Ponsaerts, P.; Van Tendeloo, V. F.; Berneman, Z. N. Regulatory T Cells and Human Disease. *Clin. Dev. Immunol.* **2007**, *2007*, 89195-1–89195-10.

(38) Germain, R. N. Special Regulatory T-Cell Review: A Rose by Any Other Name: From Suppressor T Cells to Tregs, Approval to Unbridled Enthusiasm. *Immunology* **2008**, *123*, 20–27.

(39) Wan, Y. Y.; Flavell, R. A. Regulatory T Cells, Transforming Growth Factor-Beta, And Immune Suppression. *Proc. Am. Thorac. Soc.* **2007**, *4*, 271–276.

(40) Kim, C. H. Trafficking of FoxP3+ Regulatory T Cells: Myths and Facts. *Arch. Immunol. Ther. Exp.* **2007**, *55*, 151–159.

(41) Long, E. T.; Wood, K. J. Regulatory T Cells—A Journey from Rodents to the Clinic. *Front Biosci.* **2007**, *12*, 4042–4049.

(42) Sutmuller, R. P.; Morgan, M. E.; Netea, M. G.; Grauer, O.; Adema, G. J. Toll-Like Receptors on Regulatory T Cells: Expanding Immune Regulation. *Trends Immunol.* **2006**, *27*, 387–393.

(43) Jurk, M.; Heil, F.; Vollmer, J.; Schetter, C.; Krieg, A. M.; Wagner, H.; Lipford, G.; Bauer, S. Human TLR7 or TLR8 Independently Confer Responsiveness to the Antiviral Compound R-848. *Nat. Immunol.* **2002**, *3*, 499.

(44) Gerster, J. F.; Lindstrom, K. J.; Marszalek, G. J.; Merrill, B. A.; Mickelson, J. W.; Rice, M. J. Oxazolo, Thiazolo and Selenazolo [4,5-c]-Quinolin-4-amines and Analogs Thereof. Patent WO 00/06577, 2000.

(45) Gerster, J. F.; Lindstrom, K. J.; Miller, R. L.; Tomai, M. A.; Birmachu, W.; Bomersine, S. N.; Gibson, S. J.; Imbertson, L. M.; Jacobson, J. R.; Knafla, R. T.; Maye, P. V.; Nikolaides, N.; Onyemel, F.

Y.; Parkhurst, G. J.; Pecore, S. E.; Reiter, M. J.; Scribner, L. S.; Testerman, T. L.; Thompson, N. J.; Wagner, T. L.; Weeks, C. E.; Andre, J. D.; Lagain, D.; Bastard, Y.; Lupu, M. Synthesis and Structure-Activity-Relationships of 1H-Imidazo[4,5-*c*]quinolines that Induce Interferon Production. *J. Med. Chem.* **2005**, *48*, 3481–3491.

(46) Prince, R. B.; Merrill, B. A.; Heppner, P. D.; Kshirsagar, T. A.; Wurst, J. R.; Manske, K. J.; Rice, M. J. Alkyloxy Substituted Thiazoloquinolines and Thiolonaphthyridines. Patent WO 2006/086449, 2006.

(47) Prince, R. B.; Rice, M. J.; Wurst, J. R.; Merrill, B. A.; Kshirsagar, T. A.; Heppner, P. D. Aryloxy and Arylalkyleneoxy Substituted Thiazoloquinolines and Thiazolonaphthyridines. Patent WO 2006/009826 A1, 2006.

(48) Lu, H.; Dietsch, G. N.; Matthews, M. A.; Yang, Y.; Ghanekar, S.; Inokuma, M.; Suni, M.; Maino, V. C.; Henderson, K. E.; Howbert, J. J.; Disis, M. L.; Hershberg, R. M. VTX-2337 Is a Novel TLR8 Agonist That Activates NK Cells and Augments ADCC. *Clin. Cancer Res.* **2012**, *18*, 499–509.

(49) Dowling, D. J.; Tan, Z.; Prokowicz, Z. M.; Palmer, C. D.; Matthews, M. A.; Dietsch, G. N.; Hershberg, R. M.; Levy, O. The Ultra-Potent and Selective TLR8 Agonist VTX-294 Activates Human Newborn and Adult Leukocytes. *PLoS One* **2013**, *8*, e58164–1–e58164–11.

(50) Venkataraman, S.; Barange, D. K.; Pal, M. One-Pot Synthesis of 2-Substituted Furo[3,2-*c*]quinolines via Tandem Coupling–Cyclization under Pd/C-Copper Catalysis. *Tetrahedron Lett.* **2006**, *7317–7322*.

(51) Gaddam, B.; Polsetti, D. R.; Guzel, M.; Victory, S.; Kostura, M. Substituted Pyridine Derivatives, Pharmaceutical Compositions, and Methods of Use to Treat Oxidative Stress. Patent 61/234,498 WO 2011/022216, 2011.

(52) Shukla, N. M.; Salunke, D. B.; Balakrishna, R.; Mutz, C. A.; Malladi, S. S.; David, S. A. Potent Adjuvanticity of a Pure TLR7-Agonistic Imidazoquinoline Dendrimer. *PLoS ONE* **2012**, *7*, e43612–1–e43612–11.

(53) Miller, K. A.; Suresh Kumar, E. V. K.; Wood, S. J.; Cromer, J. R.; Datta, A.; David, S. A. Lipopolysaccharide Sequestrants: Structural Correlates of Activity and Toxicity in Novel Acylhomospermines. *J. Med. Chem.* **2005**, *48*, 2589–2599.

(54) Sil, D.; Shrestha, A.; Kimbrell, M. R.; Nguyen, T. B.; Adisechan, A. K.; Balakrishna, R.; Abbo, B. G.; Malladi, S.; Miller, K. A.; Short, S.; Cromer, J. R.; Arora, S.; Datta, A.; David, S. A. Bound to Shock: Protection from Lethal Endotoxemic Shock by a Novel, Nontoxic, Alkylpolyamine Lipopolysaccharide Sequestrant. *Antimicrob. Agents Chemother.* **2007**, *51*, 2811–2819.

(55) Shukla, N. M.; Malladi, S. S.; Day, V.; David, S. A. Preliminary Evaluation of a 3H Imidazoquinoline Library As Dual TLR7/TLR8 Antagonists. *Bioorg. Med. Chem.* **2011**, *19*, 3801–3811.

(56) Tanji, H.; Ohto, U.; Shibata, T.; Miyake, K.; Shimizu, T. Structural Reorganization of the Toll-Like Receptor 8 Dimer Induced by Agonistic Ligands. *Science* **2013**, *339*, 1426–1429.

(57) Spyros, F.; BidonChanal, A.; Barril, X.; Luque, F. J. Protein Flexibility and Ligand Recognition: Challenges for Molecular Modeling. *Curr. Top. Med. Chem.* **2011**, *11*, 192–210.

(58) Wlodarski, T.; Zagrovic, B. Conformational Selection and Induced Fit Mechanism Underlie Specificity in Noncovalent Interactions with Ubiquitin. *Proc. Natl. Acad. Sci. U.S.A.* **2009**, *106*, 19346–19351.

(59) David, S. A.; Smith, M. S.; Lopez, G.; Mukherjee, S.; Buch, S.; Narayan, O. Selective Transmission of R5-Tropic HIV-1 from Dendritic Cells to Resting CD4⁺ T Cells. *AIDS Res. Hum. Retroviruses* **2001**, *17*, 59–68.

(60) Kimbrell, M. R.; Warshakoon, H.; Cromer, J. R.; Malladi, S.; Hood, J. D.; Balakrishna, R.; Scholdberg, T. A.; David, S. A. Comparison of the Immunostimulatory and Proinflammatory Activities of Candidate Gram-Positive Endotoxins, Lipoteichoic Acid, Peptidoglycan, and Lipopeptides, In Murine and Human Cells. *Immunol. Lett.* **2008**, *118*, 132–141.

(61) Alves, C. N.; Marti, S.; Castillo, R.; Andres, J.; Moliner, V.; Tunon, I.; Silla, E. A Quantum Mechanics/Molecular Mechanics Study of the Protein-Ligand Interaction for Inhibitors of HIV-1 Integrase. *Chemistry* **2007**, *13*, 7715–7724.

(62) Murphy, R. B.; Philipp, D. M.; Friesner, R. A. A Mixed Quantum Mechanics/Molecular Mechanics (QM/MM) Method for Large-Scale Modeling of Chemistry in Protein Environments. *J. Comput. Chem.* **2000**, *21*, 1442–1457.

(63) Jorgensen, W. L.; Schyman, P. Treatment of Halogen Bonding in the OPLS-AA Force Field; Application to Potent Anti-HIV Agents. *J. Chem. Theory Comput.* **2012**, *8*, 3895–3801.

(64) Antony, J.; Grimme, S. Density Functional Theory Including Dispersion Corrections for Intermolecular Interactions in a Large Benchmark Set of Biologically Relevant Molecules. *Phys. Chem. Chem. Phys.* **2006**, *8*, 5287–5293.

(65) Repasky, M. P.; Shelley, M.; Friesner, R. A. Flexible Ligand Docking with Glide. In *Current Protocols in Bioinformatics*; Schrodinger, LLC: New York, 2007; Chapter 8, Unit 8.12.

(66) Halgren, T. A.; Murphy, R. B.; Friesner, R. A.; Beard, H. S.; Frye, L. L.; Pollard, W. T.; Banks, J. L. Glide: a New Approach for Rapid, Accurate Docking and Scoring. 2. Enrichment Factors in Database Screening. *J. Med. Chem.* **2004**, *47*, 1750–1759.